Bull Earthquake Eng
DOI 10.1007/s10518-017-0257-9

ORIGINAL RESEARCH PAPER

Probabilistic seismic assessment and retrofit considerations for Italian RC frame buildings

Gerard J. O'Reilly[1] · **Timothy J. Sullivan**[2]

Received: 29 June 2017 / Accepted: 28 October 2017
© Springer Science+Business Media B.V., part of Springer Nature 2017

Abstract In recent decades, the seismic assessment of existing buildings has developed significantly from traditional objectives that focused on ensuring life safety of the building. The economic impact of the 1994 Northridge earthquake in the US due to the extensive damage suffered by buildings, in addition to the overall disruption, highlighted the need for a paradigm shift in the way in which the performance of buildings ought to be defined. This paper considers the assessment of existing Italian reinforced concrete (RC) frame buildings with masonry infill, which were typically gravity load designed (GLD) prior to the introduction of seismic design provisions in the 1970s. The assessment of GLD RC frames with masonry infill is discussed within a setting similar to that of the FEMA P58 guidelines that aim to provide practising engineers with the tools and procedures; both advanced and simplified, to quantify the performance of existing buildings in a more meaningful way that can be easily conveyed to decision makers. In this study, extensive numerical analysis was carried out on a variety of case study buildings to quantify and benchmark the performance; both in terms of expected demand and overall collapse capacity, where the impact of incorporating the potential shear failure in column members was shown to result in a reduction of up to 10% of the median collapse intensity due to the interaction with the masonry infill. Furthermore, loss estimation studies were carried out on these case study buildings to not only quantify the expected losses but also investigate ways in which shrewd retrofitting of both structural and non-structural elements can have maximum impact on the overall performance. On the contrary, it was shown that by adopting structural retrofitting schemes involving strengthening and/or stiffening of the structure in compliance with NTC 2008 requirements in these situations may actually lead to a worsening of the building performance defined in terms of expected annual loss. Overall,

✉ Gerard J. O'Reilly
gerard.oreilly@iusspavia.it

[1] Scuola Universitaria Superiore IUSS Pavia, Palazzo del Broletto, Piazza della Vittoria 15, 27100 Pavia, Italy

[2] Department of Civil and Natural Resources Engineering, University of Canterbury, Christchurch, New Zealand

Published online: 06 November 2017

this paper provides insight into the probabilistic seismic assessment and retrofit considerations for existing GLD RC frames in Italy.

Keywords Assessment · Loss estimation · Retrofitting · Collapse · Gravity-load design · RC frames

1 Introduction

Significant developments have been made in the seismic assessment of existing buildings during recent decades, with traditional objectives for assessment focusing on life safety of buildings but modern objectives looking at other performance measures such as economic losses (Calvi et al. 2014). Despite the relatively limited number of lives lost, the economic impact and overall disruption caused by the 1994 Northridge earthquake in the US suggested that a more advanced approach was needed into how performance of structures ought to be defined. Such a change came about in the US with the advent of performance-based earthquake engineering (PBEE) during the latter half of the 1990s in the form of the "Vision 2000" document (SEAOC 1995). This effectively related expected levels of building performance to different levels of earthquake intensity in order to consider not only life safety performance but also the functionality of the building as a whole, with additional consideration given to more frequent, lower intensity events. In the early 2000s, the idea of a more probabilistic PBEE assessment framework began to emerge that laid the foundations for what is now commonly referred to in the field as the Pacific Earthquake Engineering Research (PEER) Centre's PBEE methodology (Cornell and Krawinkler 2000). This approach represents a powerful methodology to quantify building performance, as not only does it consider the overall life safety of the building's occupants but it can also quantify the damage induced in all elements of the building, both structural and non-structural. In this way, the overall performance of the building can be quantified in terms of more meaningful metrics to stakeholders such as direct economic losses due to the cost of repairing the building, in addition to the anticipated downtime and other indirect sources of loss associated with returning the building to its full functionality. These performance metrics were categorised as the "3D's" (deaths, dollars and downtime) in an attempt to encompass the aspects of performance most relevant to building owners or stakeholders. This is considered a major step forward in earthquake engineering as it expresses performance in a way that is accessible to a wider audience, as opposed to utilising a parlance of demand-capacity checks and verifications mostly familiar to seismic engineers, whilst also incorporating the probabilistic nature of the problem in the overall approach.

The performance of existing reinforced concrete (RC) structures in Italy and across the Mediterranean area has received much attention in recent years. Prior to the introduction of seismic design provisions in the 1970s, structural design in Italy was primarily based on the Regio Decreto 2229/39 (Regio Decreto 1939). This provided a structural design basis in Italy for the best part of 30 years, during which a significant number of RC frames were built as part of the reconstruction at the end of the second world war. Provisions such as allowable stress values were used in design in addition to smooth reinforcing bars anchored with end-hooks in the beam-column joints, where the beam-column joint region was constructed in many cases without any transverse shear reinforcement. These frame typologies are referred to herein as gravity load designed (GLD) frames recognising that they were designed without any seismic design provisions. Over 30% of existing RC frame

structures in Italy are GLD frames (ISTAT 2011) and are quite vulnerable to damage due to seismic loading, as recently indicated following the L'Aquila event in 2009 (Del Gaudio et al. 2017).

As part of the work presented herein, extensive numerical analysis was first carried out on a variety of case study GLD structures to quantify and benchmark their performance within a PBEE framework that focuses not only on life safety but also on the quantification of direct economic losses. Recent contributions by Cardone and Perrone (2017) and Cardone et al. (2017a, b) to this subject provided information relevant to the loss assessment of GLD structures and explore ways in which retrofitting can be optimised through cost–benefit analysis. The focus of this paper is not too dissimilar, where this study looked at the impacts of retrofitting structures to meet current Italian building code requirements, both in terms of likelihood of collapse and expected annual monetary losses. Finally, some discussion into the various aspects presented in this paper is provided to highlight some of the more pertaining issues when assessing GLD RC frames within the PEER PBEE framework.

2 Case study frames

The case study frames examined consist of four different RC frames of various number of storeys, shown in Fig. 1. The strength of the reinforcing steel and concrete were 3800 kg/cm^2 (372 MPa) and 200 kg/cm^2 (19.6 MPa), respectively, as per typical design manuals in use at the time of construction. The designs were adopted from a previous study by Galli (2006) and have been designed for gravity load only specified in Regio Decreto 2229/39 (Regio Decreto 1939), along with other common construction conventions during that time, which are summarised in Vona and Masi (2004). Some typical details of these GLD frames are the lack of capacity design considerations in the beam and column members; columns with low ratios of longitudinal reinforcement (< 1.3%) as they were sized principally for axial loading, and the use of smooth reinforcing bars that affects the bonding of the reinforcement to the concrete paste resulting in a modified hysteretic behaviour compared to modern ductile detailing with ribbed bars, as outlined in O'Reilly and Sullivan (2017c). The shear reinforcement requirements implemented at the time also resulted in a very small percentage of shear reinforcement stirrups in the members and no reinforcement in the beam-column joints, which combined with the use of smooth end-hooked bars was shown to be particular vulnerable during experimental testing by Pampanin et al. (2002) and past earthquakes (EERI 2009).

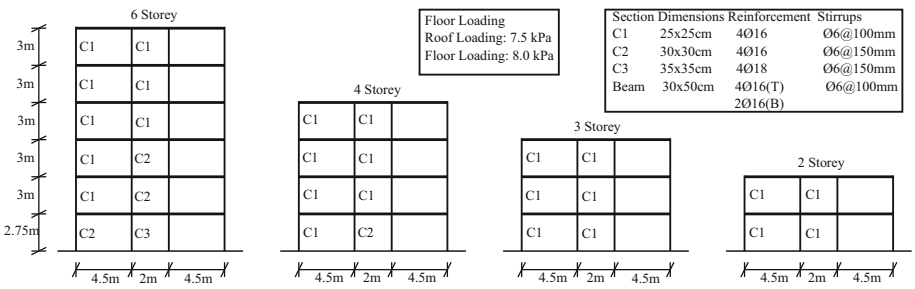

Fig. 1 Layout of case study structures adopted from Galli (2006)

While the case study structures have been designed as bare frames, it was common practice throughout Italy to insert masonry infills without considering their effects on the surrounding frame during the design process. Therefore, a number of different infill frame typologies were also investigated here to illustrate their effects on the structural behaviour and overall performance of GLD RC frames. Two different infill layouts were considered; a uniform infill throughout the height of the structure and a uniform infill layout with an open ground floor, commonly referred to as a "pilotis" frame. These pilotis frames were, and still are, quite popular throughout Italy as they offer large open areas very suitable for retail space at the ground floor. These architectural advantages are of course now well known in the earthquake engineering community to be of detriment to a structure's seismic behaviour unless properly considered, as they encourage a soft-storey response at the ground floor. In addition to the uniform infill and pilotis frames, two types of masonry infill were used and are termed "weak" and "strong" infill, as per Hak et al. (2012), corresponding to 8 cm thick single leaf infill and 30 cm thick block, respectively. These were adopted in order to illustrate the effects of different infill typology on the seismic behaviour and overall performance of the structure. Lastly, both single and double infill strut models (Crisafulli et al. 2000) were adopted to investigate the effects of modelling the potential shear failure of the columns due to the forces induced by the infill on the column members, which has been a prominent failure mechanism during past earthquakes in Italy [see review of past damage in O'Reilly and Sullivan (2017c), for example]. The effects of modelling openings such as windows or doors were not considered as part of this study. Furthermore, aspects such as the modelling of staircases and other facets associated with the three-dimensional nature of existing GLD RC frames with masonry infill are not considered here despite studies such as Cardone and Flora (2017) highlighting the potential impact of such characteristics on the behaviour of such buildings. The simplified structural configuration selected here has been chosen because the primary goal of this article is to illustrate and discuss some of the impacts different aspects of structural behaviour can have within a modern performance-based assessment of these structural typologies. Future work should aim to highlight how stairs and 3D characteristics also affect modern measures of seismic performance.

For each of the case study structures described above, a numerical model was built in OpenSees (McKenna et al. 2000) using the numerical modelling approach outlined in O'Reilly and Sullivan (2015, 2017c), and discussed in more detail in O'Reilly (2016). The beam and column elements were modelled using a lumped plasticity element, where the different parameters required for the beam-column element model were determined from the calibration with existing experimental test data to adequately capture the behaviour of the older GLD RC frames discussed here. To incorporate the effects of masonry infill, the equivalent diagonal strut models outlined in Crisafulli et al. (2000) were adopted and the proposals of Sassun et al. (2015) for the hysteretic backbone of these struts were utilised. As detailed in O'Reilly and Sullivan (2017c), the potential shear failure of the column members was considered through a shear hinge placed at the ends of the columns so that the additional shear force transferred from masonry infill on to the columns could be incorporated. The beam-column joints were modelled using a zero-length hinge at the joint centres to characterise the vulnerability of these to brittle shear failure as a result of no transverse reinforcement in the joint region. Similar to the beam-column elements, the various parameters defining the model were taken from the calibration study described in O'Reilly and Sullivan (2017c). A tributary width of 4.5 m was adopted and the floor system is modelled using a rigid diaphragm, which was deemed a reasonable assumption

for the "laterizio" floor systems that were quite common in Italy at the time of construction.

3 Characterising the behaviour

3.1 Static pushover analysis

The first set of analyses conducted on the case study frames were static pushover (SPO) analyses, where a set of lateral forces were applied to the numerical models (in proportion to the product of the mass and first mode shape vectors) and scaled incrementally. Figure 2 shows the SPO curves where the base shear coefficient (base shear normalised by the total structure weight) is plotted versus the roof displacement. As is immediately evident from Fig. 2, the presence of masonry infill significantly modified the lateral behaviour of the frames, which can be seen through the increased initial stiffness and peak base shear capacity. In relation to the number of storeys, the peak base shear coefficient tended to reduce with increasing storey number. This is expected when one considers that the peak base shear capacity tends to be limited by the capacity of a single storey that forms a mechanism and remains somewhat constant, meaning that when normalised by the total structure weight it decreases for taller structures. In current practice, it is understood that masonry infills are often neglected in the assessment of existing buildings and in the design of retrofit interventions. Clearly, by comparing bare frame and infilled frame responses, this work shows that such an approach is inadequate. Since practitioners may or may not consider the impact of infills when doing retrofit design, there is uncertainty as to the retrofit measures that are most representative of current practice. However, this issue has been overcome in this work by examining a range of possible retrofit options, and for the structural retrofit options it was assumed that gaps would be provided around the infills thus avoiding the need to consider infills further within the design of the structural retrofit measures, which will be further discussed in Sect. 5.

Comparing the response of frames without infill modelled and pilotis infill frames, in each case the presence of the masonry infill in the upper storeys tended to increase the initial stiffness of the structures but entails a similar maximum base shear capacity since the governing mechanism was a column-sway mechanism at the ground floor. For the case of the pilotis frames, a relatively consistent behaviour between each of the different structures can be observed. This is seen both through the base shear coefficient at yield as

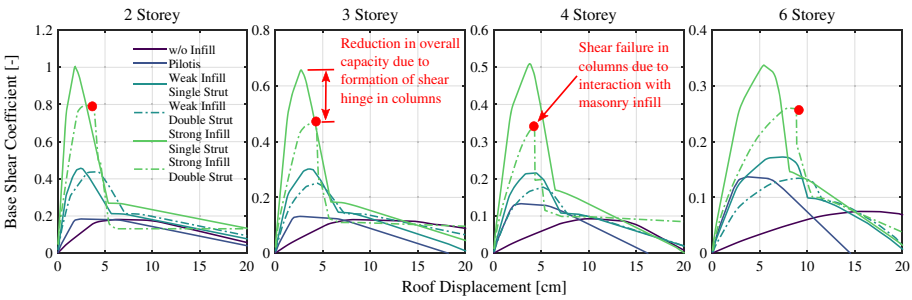

Fig. 2 SPO curves showing base shear coefficient versus roof displacement of the structure for each modelling variation

well as the overall displacement capacity, where the displacement tends to reduce with increasing number of storeys due to the growing influence of P-Delta effects. Compared to the other configurations, the pilotis buildings exhibit a relatively bilinear behaviour before degrading and differ from the other infill typologies since they do not possess the characteristic peak base shear followed by a significant drop in base shear for the infilled frames. Compared to the frames without masonry infills, the pilotis frames show a stiffer and more consistent behaviour as they are characterised by little deformation in the upper levels and a concentration in deformation at the open ground storey.

Comparing the modelling of the shear behaviour of the column members in Fig. 2, the initial stiffness of the single and double-strut infill models for both weak and strong infill typologies is seen to be quite comparable, although the double-strut models tended to be slightly longer due to an additional shear flexibility in the columns whereas the diagonal struts were connected to the surrounding frame. This additional flexibility was also reflected in the eigenvalue analyses, where considering the double-strut infill model resulted in an increase of up to 12% in the first mode period of vibration for the fully infilled frames with respect to corresponding single-strut cases (see Table 1). One of the main advantages of incorporating the shear behaviour and failure of the columns due to the interaction with the masonry infill is that this damage mode can be directly simulated during analysis, as illustrated in Fig. 2, and its influence on the actual peak response can be directly incorporated and would not require post-processing checks to determine whether the shear demand in the columns is critical or not.

3.2 Incremental dynamic analysis

The next set of analyses that were conducted on the case study frames were IDA (Vamvatsikos and Cornell 2002), where a set of ground motion records were scaled incrementally to examine the response of the structure with respect to intensity. The intensity measure (IM) used was the spectral acceleration at a conditioning period T*(Sa(T*)) where T* corresponds to the first mode period of vibration of the structure (T_1), which are listed in Table 1. Comparing the first mode periods of each structural typology, the impact of the presence of the masonry infills, with respect to the models without, is immediately obvious. The periods were much shorter and the relative strength of the masonry infill was also seen to play an important role. The use of a double strut model to capture the potential shear failure of the columns was also seen to have a non-negligible effect on the modal properties, as noted in the previous section. For the pilotis frame structures, it was seen how there was relatively little difference between the 3, 4 and 6 storey buildings, despite the

Table 1 First mode period of vibration for each of the case study structures

Structural typology	2 Storey (s)	3 Storey (s)	4 Storey (s)	6 Storey (s)
w/o infill	0.80	1.15	1.44	1.86
Pilotis frame	0.60	0.71	0.69	0.70
Infilled frame (weak masonry, single strut)	0.25	0.37	0.44	0.62
Infilled frame (weak masonry, double strut)	0.25	0.37	0.47	0.69
Infilled frame (strong masonry, single strut)	0.15	0.21	0.29	0.41
Infilled frame (strong masonry, double strut)	0.16	0.24	0.30	0.46

buildings increasing in overall mass. This was attributed to the first mode of the pilotis frames being a soft-storey mechanism at the ground storey and due to the fact that the column sizes at that level increased in size; and subsequently stiffness, the relative ratio of increased mass to stiffness was maintained to give rather small changes in first mode period. A Rayleigh damping model was adopted by applying 5% of critical damping to the first and third modes of vibration. The record set used to track the evolution of damage and response in the structure was the far-field set given in FEMA P695 (FEMA P695 2009). It is acknowledged that the use of a single set of ground motion records scaled using IDA raises some issues regarding hazard consistency at the different intensities. As such, the results presented herein are considered within a comparative context and is noted that for application to actual existing buildings, a more rigorous record selection approach, such as that provided by Baker and Lee (2017), for example, is recommended. Nevertheless, it is anticipated that even with a more sophisticated record selection methodology the overall conclusions of the work presented herein in Sects. 6 and 7 would not change.

In terms of actual results, each frame and modelling variation was analysed and the pertaining demand parameters examined with respect to increasing intensity. This results in a large amount of numerical analysis output that, in the interests of being brief are omitted here [but detailed further in O'Reilly (2016)] and the results are summarised in terms of their medians for general comparison. Figure 3 plots the median values of maximum peak storey drift (PSD) for the frames, while Fig. 4 plots the maximum peak floor acceleration (PFA). Since the conditioning period, T* is different for each structure, the IMs are not directly comparable by themselves. The vertical axis of Fig. 4 therefore reports the spectral acceleration at the fundamental period of vibration normalised by the 2500-year return period spectral acceleration ($S_{a,2500years}$) at the respective conditioning periods for a given site, chosen here to be the site of Napoli, which will be discussed further in Sect. 4. This normalisation allowed the median values from the different structural typologies to be compared in a more meaningfully way. Some median plots were cut short at higher intensities where the probability of collapse exceeds 90%, as this resulted in difficulty obtaining a representative median demand for the limited number of non-collapsing records. The term "conditioned on no collapse" refers to how the median plots were computed using cases where the ground motion records that did not exceed the collapse criterion discussed in Sect. 3.3 and did not experience numerical convergence issues to prevent the completion of analysis. By making such a distinction, the total expected losses, $E[L_T|IM]$, arising from both the expected losses conditioned on collapse; or building replacement cost, and no collapse, $E[L_T|NC, IM]$, cases will be computed in Sect. 4 as follows:

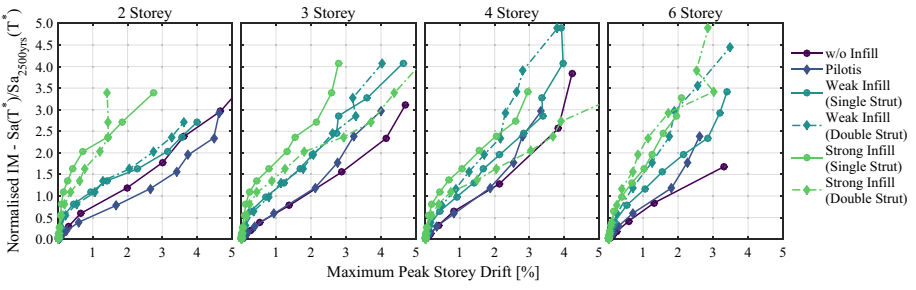

Fig. 3 Median value conditioned on no-collapse of the maximum PSD over all floors at each normalised intensity for each frame

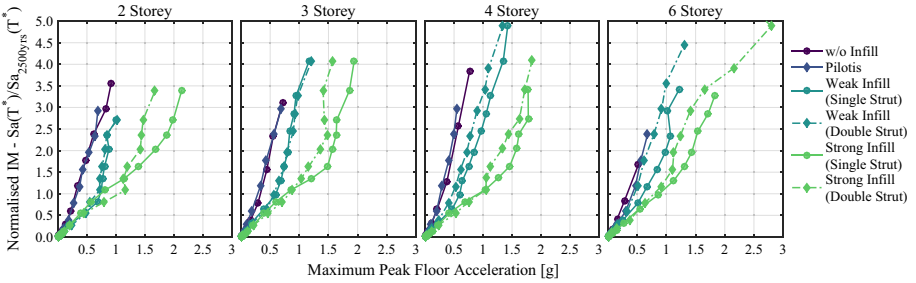

Fig. 4 Median value conditioned on no-collapse of the maximum PFA over all floors at each normalised intensity for each of the case study structures

$$\mathrm{E}[\mathrm{L_T}|\mathrm{IM}] = \mathrm{E}[\mathrm{L_T}|\ \mathrm{NC},\ \mathrm{IM}](1 - \mathrm{P}[\mathrm{C}|\mathrm{IM}]) + \mathrm{P}[\mathrm{C}|\mathrm{IM}] \times \mathrm{RC} \quad (1)$$

where P[C|IM] represents the probability of collapse for a given level of IM, the labels C and NC denote the collapse and no collapse cases, respectively, and RC represents the replacement cost of the building.

Comparing the general response of the frames in terms of bare and infill frame typology, the bare frame displayed a much higher drift demand than that of the infilled frame due to the presence of the masonry infill. In terms of floor acceleration demand, the infill frames showed a much higher demand than the corresponding frames without infill modelling, which was to be expected. Again, it was seen how the strength of the masonry infill influences these floor accelerations with the stronger infill resulting in a higher acceleration demand than that of the weaker infill. Finally, comparing the response of the single-strut and double-strut masonry infill frames, it is evident that in terms of maximum PSD demand, the double-strut models showed a general increase with respect to the single-strut models, which was consistent with the findings of the SPO analysis, whereas there was no significant difference between the single and double strut models, although it could be argued that the use of double-strut led to a slight decrease in the maximum PFAs.

3.3 Collapse assessment

3.3.1 Collapse fragility from IDA

For each ground motion record of the IDA, analysis results were subjected to a continuous check on the current maximum drift in the structure at each moment in time during the analysis. If the current maximum drift exceeded a prescribed maximum storey drift capacity, the analysis was terminated at that point and the record marked as a collapse case. The prescribed storey drift limit for this work was 10%, which has been defined from sensitivity studies and also been used in past studies examining collapse, such as Gokkaya et al. (2016). The definition of such a drift limit was implemented during numerical analysis so that when a structure accumulates excessive drift demand and begins to collapse (i.e. the IDA trace begins to flatline), there was a quantitative definition of collapse at a global structural level that the current drift could be checked against without the need to individually check the various structural members' chord rotations etc. Sensitivity analyses on the value of this drift limit showed that when varying its value from 1% through to 11% peak storey drift, the median collapse intensity and associated dispersion began to converge to stable values around a drift limit of 5%, meaning that the definition of a higher

drift limit of 10% enabled collapse to be identified with a good degree of confidence. Interestingly, this convergence limit of around 5% corresponds well with the limit of 4.36% outlined in Rossetto and Elnashai (2003) for European infilled RC frames. However, it must be stated that this storey drift capacity check was only applied to structures with fully converged response and was not applied to situations where, for various reasons, a numerical model may be unable to achieve convergence for a particular record without having entered into the predefined collapse storey drift range. These situations were removed from the analysis results and were not used any further.

Using the above definition of collapse, the IDA returned a number of collapses and a number of fully converged and completed analyses for each intensity. The ratio between these two was used to describe the probability of collapse for a given intensity and this was then used to construct the collapse fragility of the structure, whose application to fitting fragility functions using truncated data sets has been described in Baker (2015). The fragility functions were fitted assuming a lognormal distribution that was checked using the Lilliefors goodness-of-fit test at the 5% significant level. Figure 5 shows these fitted collapse fragilities for the case study structures. Again, the IM for each frame is normalised to allow relative comparison between the different structural typologies. It is important to note that the median and dispersion in the collapse fragility functions described here account for record-to-record variability ($\beta_{RC,IM}$) only and do not incorporate the adjustments proposed in O'Reilly and Sullivan (2017b) to account for modelling uncertainty. The adjustment prescribed in FEMA P695 for spectral shape were also omitted as the factors provided in FEMA P695 were developed for ductile structures in the US and are not necessarily applicable here.

As seen in Fig. 5, the trends followed the observations in the SPO results presented in Sect. 3.2, where the structures with full masonry infill tended to have a much higher normalised median collapse intensity than pilotis frames and frames without infills modelled. Comparing the collapse fragility of the frames without infill modelled and pilotis

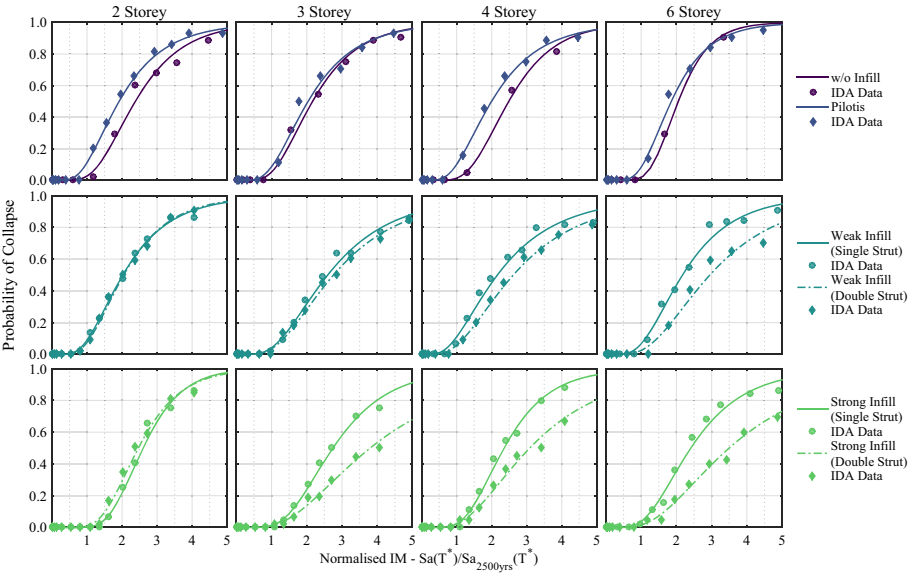

Fig. 5 Collapse fragility curves for each of the structures

frames, the pilotis frames tended to have a lower normalised median collapse intensity and comparable dispersions. This agrees well with past earthquakes where the presence of an opening ground floor tended to result in many instances of collapse.

Another important point of observation is the comparison between the response of the single and double-strut models of the masonry infill structures. The double strut infill model allowed the consideration of the shear flexibility and possible failure of the columns during the analysis, where the inclusion of such a double strut model in SPO analysis revealed the shear failure in the column members for strong infill, whereas for weak infill an increased flexibility of the frames was observed. The impacts of this on the collapse fragility is of particular interest given the prevalence of this failure mode in past earthquakes in Italy. The IDA results showed that the double-strut models tended to report a higher maximum PSD than their single-strut model counterparts, which was due to the additional flexibility of the double-strut frames. However, comparing the median collapse intensities, for both weak and strong masonry infill typology, the median collapse intensity of the double-strut is not always lower than the corresponding single strut model and in some cases, slightly higher than the corresponding single-strut model (e.g. three-storey weak infill and four and six-storey strong infill). This is a peculiar observation at first that somewhat contradicts the overall observations of the IDA results, since the double-strut models were actually more vulnerable in the sense that they showed higher deformation for a given intensity when compared in terms of the maximum of the peak profiles. However, while the normalised median collapse intensities were slightly higher for the double-strut models, this does not necessarily imply an increased collapse resilience. The dispersion of the collapse fragility function must also be considered alongside the annual rate of exceedance of their respective IMs. Therefore, a more appropriate comparison of the relative collapse performance would be through integrating over the respective hazard curves to compute the mean annual frequency of collapse, or by computing the probability of collapse for a given return period intensity, as will be discussed further in Sect. 4.1.

3.3.2 Collapse fragility using the SPO2IDA tool

While the previous section described how the collapse fragility can be computed using the data obtained from truncated IDA, a simpler way is examined here using the SPO2IDA tool described by Vamvatsikos and Cornell (2005). This tool takes the SPO curve and, by defining a multi-linear backbone, determines an IDA trace using a series of empirical expressions related to the definition of the input multi-linear backbone. This approach worked remarkably well for a tool of its simplicity in the illustrative examples discussed in Vamvatsikos and Cornell (2005), with the 16th and 84th fractile traces also being well represented. As such, it is of interest as to whether the collapse fragility function of GLD RC frames using such a simplified method is possible. If it works well, it could be combined with more simplified methods, such as those described in Priestley et al. (2007), for example, so that both the performance conditioned on collapse and no collapse of a structure can be estimated with reasonable accuracy, without the necessity of time consuming numerical modelling and analysis. Given the above, the SPO2IDA tool was applied to each of the case study frames to examine the applicability to GLD frames with masonry infills. These were compared in terms of both the median collapse intensity and dispersion. The SPO backbones from Sect. 3.1 were provided as input to the spreadsheet tool and the

resulting median intensity and dispersion compared to those observed using IDA in Sect. 3.2.

Figure 6 illustrates the comparison between the two approaches. Regarding the dispersion, the SPO2IDA tended to underestimate the dispersion in most cases; especially for the infilled frames. In the case of the median collapse intensities, the frames modelled without infills and the pilotis frames tended to be estimated reasonably well by SPO2IDA, albeit a little conservative, whereas the infill frames were not well represented at all. This discrepancy arose due to the fundamental difference in behaviour of the frames, where for the frames modelled without masonry infill and the pilotis frames, the first mode dominated the response and a first mode based SPO was representative of the dynamic response of the structure, as per the requirements of SPO2IDA outlined in Vamvatsikos and Cornell (2005). In the case of the infilled frames, however, the first mode response was not necessarily representative over the full ductility range as the exhaustion of the masonry infill capacity at one or more storeys resulted in a fundamental change in response and subsequently, a period shift in addition to a modification of the first mode of vibration. The presence of the infill alongside the RC frame resulted in the presence of two "yield" displacements of the frame corresponding to the yielding of the infill and the yielding of the RC frame. In fitting the SPO2IDA curve to the SPO backbone, the first yield point to be matched in the case of the infilled frames was the peak capacity, which in the original definition of the hysteretic behaviour by Vamvatsikos and Cornell (2005) represents the point from which the system ductility is measured; meaning that the frame ductility was being expressed as a function of the infill peak force displacement. This represents a confusion in definitions for which the SPO2IDA was not initially developed. As a consequence, the error in estimating the median collapse intensity should be a somewhat expected result. Such an error in estimating the collapse fragility for GLD frames with masonry infill using SPO2IDA was also recently observed by Cardone and Perrone (2017), for example, where the median collapse intensity was noted to be much lower when compared to the number of actual collapses seen from NRHA, which agrees with the findings of Fig. 6.

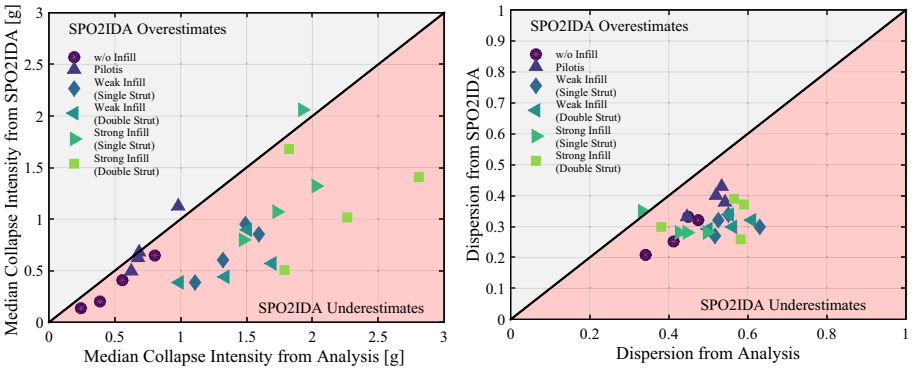

Fig. 6 Comparison of the median collapse intensity (left) and dispersion (right) computed from NRHA with that estimated using the simplified SPO2IDA tool for the various structural typologies

4 Assessment of case study structures

This section discussed the assessment of the different case study frames previously analysed. This was done both in terms of the life safety requirements outlined in current codes such as NTC 2008 (NTC 2008), in addition to examining the direct monetary losses in the structures through the detailed consideration of the damageable elements. Following the assessment of the existing structures, different approaches of structural and non-structural retrofitting were explored and their implications will support the guidance for the identification of retrofit solutions, discussed in Sect. 5.

4.1 Collapse assessment

In order to evaluate the likelihood of collapse for each of the structures examined here, the collapse requirement outlined in FEMA P695 (2009) was adopted to check that the probability of collapse did not exceed a prescribed level of 10% at the maximum considered event (MCE) intensity. This was done by taking the collapse fragility functions for each of the case study structures developed in Sect. 3.3, along with the proposed adjustments to median and dispersion to account for modelling uncertainty proposed in O'Reilly and Sullivan (2017a, b), to compute the probability of collapse at the MCE intensity level. The site location of the structures was chosen to be in Napoli, with a corresponding INGV database ID number of 32,979, where the INGV database (Montaldo and Meletti 2007) provides seismic hazard data for a number of periods of vibration and return periods throughout Italy. The NTC 2008 collapse prevention requirement is specified as 5% probability of exceedance in the specified reference period, which can be taken to be 50 years, assuming a Class II usage. This gives a return period of 975 years assuming a Poisson distribution. Contrasting this value to that typically adopted in FEMA P695, which utilises a return period of 2475 years, the intensity is somewhat lower. This difference may be due to the disparities in expected seismicity between Italy and California, although this is not the focus of the study described herein. In order to maintain consistency with the collapse prevention return period prescribed in NTC 2008 for Italy, a return period of 975 years was adopted here and the probability of collapse at this intensity is determined for each frame and checked against the prescribed limit of 10%.

The top of Fig. 7 shows this comparison for the site location in Napoli, where the structures met the collapse criterion. However, as the GLD RC frames analysed here have no seismic provisions incorporated into the design process, they are anticipated to be representative of RC frame structures throughout Italy constructed prior to 1970. As such, an additional site of higher seismicity located in L'Aquila (INGV ID 26306) was also investigated and its results shown in the bottom of Fig. 7. Comparing the performance of these structures if they were located in L'Aquila, the performance criterion was not satisfied for many of the structures and would be deemed to require structural intervention to improve their performance, whereas those located in Napoli would not. This was one of the main aspects examined in this study, where depending on the collapse risk, the implications of different retrofitting measures on the performance defined in terms of monetary loss were examined. The collapse criterion was ultimately that which must take precedence, as this represented the most fundamental aspect of performance, whereas mitigating excessive monetary losses represents a further consideration. Cardone et al. (2017a, b) also highlighted this aspect during a cost–benefit study where they noted that for many existing GLD RC frames in Italy, these may be characterised by a low collapse risk owing to the

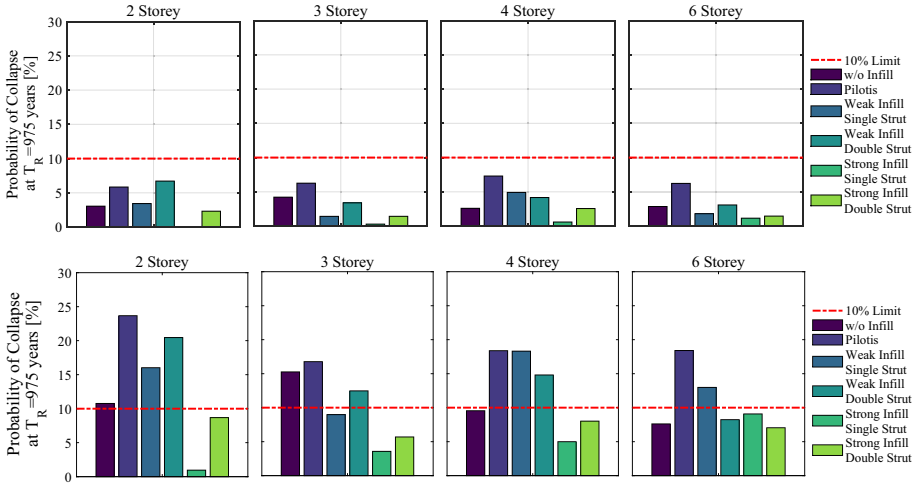

Fig. 7 Probability of collapse for the different case study structures checked at TR = 975 years to not exceed a value of 10%, as per the FEMA P695 (2009) guidelines, for structures located in Napoli (top) and L'Aquila (bottom)

low level of seismic hazard at a given site and it would be therefore reasonable to target the reduction of economic losses. In summary, the performance of the structures at the chosen site location were shown to satisfy the collapse criterion and their expected monetary losses incurred in these are examined in the following section.

Finally, further to earlier discussion in Sect. 3.3.1, the results shown in Fig. 7 give a better idea of the relative collapse performance of the different structural typologies. It is seen how the pilotis configurations tended to have the highest probability of collapse for a given return period, which agrees with the observations of past earthquakes in Italy. Furthermore, the relative performance of the infilled frames using either single or double equivalent diagonal strut models to account for potential shear failure in the columns can be evaluated. It is seen from Fig. 7 that the double strut models did, in fact, tend to return a higher probability of collapse for a given return period. Recall that a higher normalised median collapse intensity was reported in Sect. 3.3.1 but these results show that the higher normalised median intensity does not necessarily mean the structure is more resilient to collapse. In fact, Fig. 7 shows this to be on the contrary and was an expected result when considering the prevalence of such shear failures in column members due to frame-infill interaction following past earthquakes in Italy.

4.2 Loss estimation

This section builds on the analysis from Sect. 3 where, in combination with an assumed inventory of damageable structural and non-structural elements, the expected loss versus intensity of each structure examined was computed and considered as part of a general vulnerability assessment of the different structural typologies. The following subsections first discuss some of the assumptions made regarding the damageable inventories used for the loss estimation, such as the types of damageable elements, assumed fragility functions and associated repair cost functions. Losses at various intensity levels were computed and a time-based assessment conducted. It should be noted here that this study focused on direct

economic losses that arise from repair and replacement of damaged components, where other aspects such as indirect losses and downtime were not discussed and deemed beyond the scope of this article.

4.2.1 Structural and non-structural element inventory

For each of the case study structures described in Sect. 2, in order to undertake the loss estimation according the PEER PBEE framework, the following pieces of information were required (1) the quantity of each damageable element; (2) an appropriate set of fragility functions to assess the probability of each damage state for a given demand; (3) and an appropriate set of repair cost functions to estimate the expected repair costs associated with each damage state. Table 2 lists this information making reference to sources in the literature for both the fragility functions and repair cost functions. It is noted here that the entire damageable element inventory is assessed using the structural analysis

Table 2 Inventory list of the damageable structural and non-structural elements with the corresponding assumed quantities, fragility and repair cost functions for each floor of the case study structures

Damageable elements	Quantities	Fragility and repair cost functions
Structural elements		
Non-ductile columns	12	Cardone (2016)—DWC (continuous)
Exterior beam-column joints	14	Cardone (2016)—EWJs (end hooks)
Interior beam column joints	10	Cardone (2016)—IWC
Exterior masonry infill (no windows)	60 m^2	Cardone and Perrone (2015)—EIW
Exterior masonry infill (windows)	60 m^2	Cardone and Perrone (2015)—EIW_w
Interior masonry partitions (doors)	24 m^2	Cardone and Perrone (2015)—IP_d
Non-structural elements		
Internal gypsum partitions	100 ft	FEMA P58-3 (2012)—C1011.001a
Internal gypsum partition wallpaper finish	100 ft	FEMA P58-3 (2012)—C3011.001a
Internal gypsum partition ceramic tile finish	100 ft	FEMA P58-3 (2012)—C3011.002a
Suspended ceilings	1065 ft^2	FEMA P58-3 (2012)—C3032.001b
Cold water piping	1000 ft	FEMA P58-3 (2012)—D2021.011a
Cold water piping bracing	1000 ft	FEMA P58-3 (2012)—D2021.013b
Hot water piping	1000 ft	FEMA P58-3 (2012)—D2022.011a
Hot water piping bracing	1000 ft	FEMA P58-3 (2012)—D2022.011b
Glazed windows	10	Sassun (2014)—Glazing Panels 1.0 × 2.5 m
Lighting	15	FEMA P58-3 (2012)—C3034.001
Elevator	1*	FEMA P58-3 (2012)—D1014.012
HVAC in-line fan	2	FEMA P58-3 (2012)—D3041.002a
HVAC ducting	2	FEMA P58-3 (2012)—D3041.011a
HVAC diffusers	2	FEMA P58-3 (2012)—D3041.031a
HVAC fan	1**	FEMA P58-3 (2012)—D3041.101a
Chiller	1*	FEMA P58-3 (2012)—D3031.011a
Air handling unit	2**	FEMA P58-3 (2012)—D3031.021a

* At ground level only

** At roof level only

results from the single direction analysed of the case study structures analysed—a simplifying assumption that assumes that similar structural response is to be expected in both directions of the structure and that reasonable estimates of economic loss can be obtained for regular structures such as those examined here.

Quantities of each element were estimated based on the size of structures where the usage could be considered that of a public-school building. The types and typical quantities of each of the elements were based on judgement following building surveys conducted on a number of school buildings in Italy (O'Reilly et al. 2017a, b). Another more general note regarding the non-structural elements in the structure is that these elements were intentionally selected as having no seismic design provisions, such as bracing of the ceiling or piping systems, or protection of acceleration sensitive equipment via special snubbers etc. This was done so as to be more representative of the observed non-structural detailing of older RC buildings in Italy. Section 5 looks to investigate the relative impact of improving these non-structural element details on the overall performance of the structure.

Many of the assumed fragility and repair cost functions were taken from the PACT fragility library (FEMA P58-3 2012), which has been largely developed for use in the US. In order to make the repair cost functions applicable to older Italian structures, an equivalent conversion between average construction costs in the US and Italy for 2013 was utilised. This conversion was carried out with the assistance of a consulting engineering firm in Italy, where the costing manuals from both countries were used to give the best estimation of the repair cost conversions. The resulting average ratio between the two construction costs in 2013 was found to be 1.22 times the US cost, which also takes into account the currency conversion from the same year. While it would be ideal to derive such costing functions from scratch using Italian costing manuals, such an approach was deemed beyond the scope of this work due to the vast amount of information and experience required. As such, the equivalent conversion utilised here may be thought of as a suitable compromise for the comparative studies presented herein and is not envisaged to have an effect on the overall conclusions of this work.

In addition to the repair costs, an appropriate estimate of the replacement cost of each structure was required so that the contribution to the expected losses from the collapsing cases can be estimated. To estimate these replacement costs, available information in Italy following the 2012 Emilia–Romagna earthquake was used to find the typical cost of replacing a building per unit area in addition to the costs of demolition and removal of debris. Again, with the aid of an Italian consulting engineering firm, the average replacement costs were found to be €1805.75 per m^2 and an additional €95.50 per m^2 for demolition and removal of the existing structure. In addition to the replacement cost of the building, a threshold value was set to define the ratio of expected direct loss to the replacement cost that a stakeholder would typically elect to demolish the building rather than repair the existing, heavily damaged one. FEMA P58-1 (2012) suggests a value of 40%, although Cardone and Perrone (2017) note that according to Dolce and Manfredi (2015), slightly higher cost ratios of between 60 and 75% of the replacement cost were sustained following the L'Aquila earthquake of 2009. An interesting side note from a study by Elwood et al. (2015) following the Canterbury earthquakes of 2011 and 2012 in New Zealand also present some further insight into threshold values for the demolition of existing RC buildings. They note that over 50% of the structures noted to have a damage ratio of between 2 and 10% were demolished. Elwood et al. (2015) went on to say that this notably low ratio can be attributed to a more legislative decision whereby the older RC structures were considered more "earthquake prone" and were more likely to be demolished, regardless of the actual damaged state of the structure. This highlights the

uncertainty in such a threshold value that arises not only from engineering-based decisions on acceptable levels of structural and non-structural damage but also on the legislative aspects that come into play in the post-earthquake aftermath. Using the information outlined in Cardone and Perrone (2017) for the case of Italy, however, a threshold value of 60% was adopted for all analysis discussed herein. This value considers the ratio of the direct losses to the overall replacement cost, where if the indirect losses were to be considered, this value could be expected to somewhat lower. However, since this study focused on direct losses, the adopted value of 60% was considered reasonable. Residual drifts were also incorporated by adopting a residual drift fragility curve with a median value of 1.5% maximum residual story drift with a dispersion of 0.3, as per Ramirez and Miranda (2009), to determine the situations where demolition would also be likely due to excessive residual drifts in the structure. Lastly, the adjustments to the collapse median and dispersion in addition to the dispersion of the PSD and PFA to account for modelling uncertainty were adopted from the proposals of O'Reilly and Sullivan (2017b) for GLD RC frames with masonry infill. In terms of collapse, this involved reducing the median collapse intensity and increasing the dispersion to account for the uncertainty in the numerical modelling. Additionally, the overall dispersion associated with record-to-record variability for both the PSD and PFA has been inflated to account for the added dispersion in the demands due modelling uncertainty. These values were developed in a quantification study by the authors (O'Reilly and Sullivan 2017a) using a numerical modelling approach that was calibrated to available experimental test specimens (O'Reilly and Sullivan 2017c). The study (O'Reilly and Sullivan 2017a) focused on older GLD RC frames with masonry infill with non-ductile response mechanisms in contrast to the values provided in guidelines, such as FEMA P58, that were developed in a similar fashion but for structural typologies typical of modern ductile buildings in the US.

4.2.2 Results

Similar to the presentation of the IDA results, the loss estimation of each case study structures resulted in a vast amount of information. As such, summary plots of the expected losses versus normalised intensity (referred to herein as vulnerability functions) are presented together whereas more specific plots of individual cases related to the discussion are presented later to provide further details on the different comments and observations being made. Figure 8 presents the vulnerability functions for each of the case study structures in addition to a breakdown of the expected losses conditioned on no collapse for the two demand parameters examined here.

By first comparing the vulnerability functions in Fig. 8, which plot the total expected loss from both collapsing and non-collapsing cases normalised by the replacement cost of the structure versus the normalised IM, the expected losses showed similar trends. This has also been noted recently by Cardone et al. (2017a, b) for a number of fully infilled GLD RC frame buildings with number of storeys ranging from four to eight. Furthermore, it is noted that the results presented here echo the findings of the aforementioned study by Cardone et al. (2017a, b) who note a linear trend in expected loss with increasing intensity which may be useful in the development of more simplified loss estimation approaches. For the pilotis frames, the contributions of the drift sensitive elements to the expected losses were capped by the same amount for each structure. This was due to the formation of a soft-storey in the ground floor in each case meaning that the expected loss due to PSD tended to be capped by the repair cost associated with that floor. For the PFA sensitive losses, however, a similar trend can be observed where the expected losses tended to be capped for

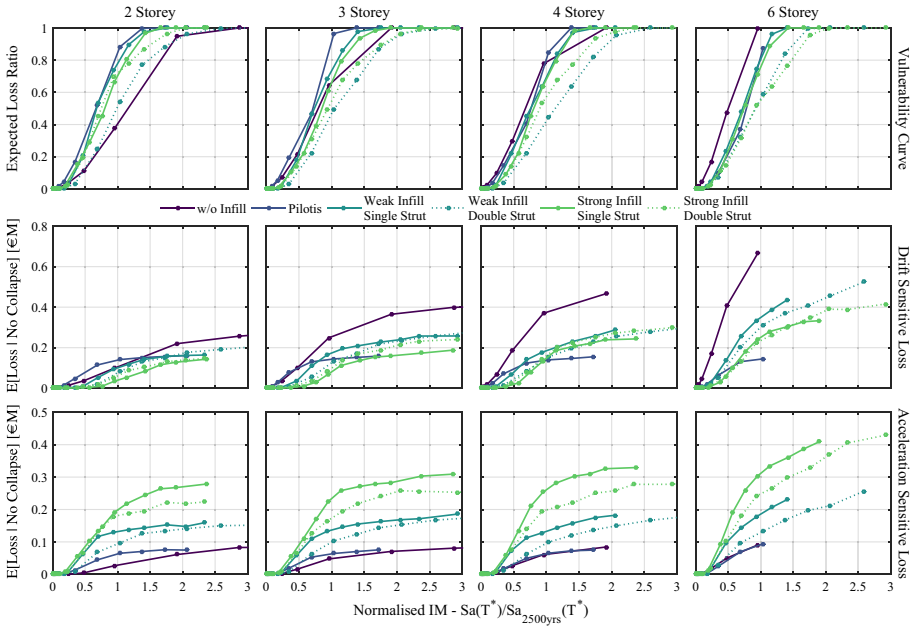

Fig. 8 Expected loss versus normalised intensity and disaggregation of expected losses in terms of drift demand (middle row) and floor acceleration demand (bottom row)

each of the pilotis structures, although a slight increase in the case of the six-storey frame was noted. This may be due to the possible increased contribution of higher mode effects on the structure resulting in a slightly increased PFA profile and hence induced more damage to acceleration-sensitive components in the upper storeys. In addition, the increased column size at the ground floor of the six storey pilotis frames meant that the acceleration at storey yield was increased slightly, meaning the soft-storey allowed the transmission of a slightly higher PFA to the upper floors.

Comparing the above observations with those of the infilled frames, Fig. 8 shows that in the case of fully infilled structures the PFA sensitive elements began to dominate the expected losses of the structures, which makes intuitive sense as the addition of masonry infill tended to result in a stiffer structure leading to higher floor acceleration than a corresponding frame modelled without masonry infill that tended to be more flexible. This highlighted the principal differences in the behaviour of the frames with no infill modelling and fully infilled frames, not just in terms of dynamic response to ground motions, but also the difference in the most vulnerable components in the respective structures. These observations regarding the dominance of the acceleration-sensitive elements to the overall damage have been observed during past events in Italy, where EERI (2009) reported that while many older RC structures with infills performed well from a structural integrity and life safety standpoint, extensive damage to the interior elements such as infills, ceilings and piping were observed following the L'Aquila event in 2009, for example. One case highlighted in EERI (2009) was for the City Planning Offices in L'Aquila, which exhibited very little exterior building damage, but is seen from Fig. 9 to have significant damage to these aforementioned non-structural elements.

Some other observations regarding the influence of the infill typology and modelling techniques can be drawn from the plots of Fig. 8, where the use of a double strut model for

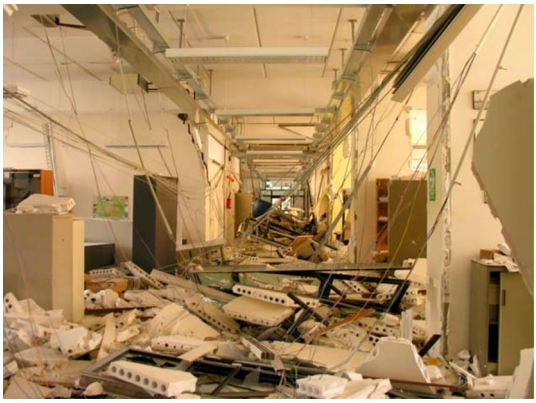

Fig. 9 Illustration of the observed non-structural element damage to the City Planning Offices in L'Aquila, whose infilled RC frame building was noted by EERI (2009) to have sustained very little detectable damage to the exterior

both infill typologies resulted in a similar trend in overall expected loss accumulation, with the double strut models tending to be slightly more vulnerable in each case. However, the breakdown of expected losses in terms of demand parameter, presented in Fig. 10, shows that the single strut models accumulated more acceleration sensitive losses while the double strut models tended to accumulate more in the drift sensitive elements. This conclusion agrees with the overall findings of the SPO and IDA results that previously showed how the structures with double strut models tended to be slightly more flexible than their single strut counterparts. Again, this highlights the importance of proper modelling of the anticipated shear behaviour in the columns.

4.3 Time-based loss assessment

The EAL is obtained by integrating the vulnerability functions with a mean hazard in what is termed a time-based assessment. Using the site hazard, the expected loss can be computed. The resulting EAL for each of the case study frames are presented in Fig. 11, with

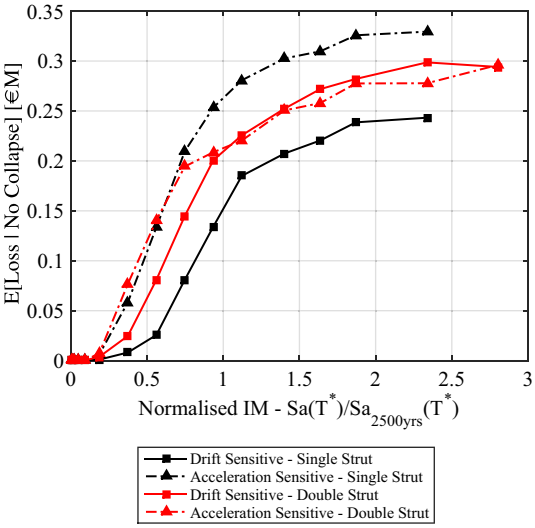

Fig. 10 Comparison of the expected loss as a function of demand parameter for the three-storey frame with strong infill modelled using both single and double strut infill approaches

the values ranging between around 0.2 and 1.3% the replacement cost of the building depending on the structural typology. An overall decrease in EAL with respect to number of storeys was also observed, which is consistent with previous studies (Calvi et al. 2014). In addition, it was seen that with respect to single strut models, the infilled frames modelled with double struts tend to report higher EAL, possibly due to the higher probability of rate of collapse reported in Sect. 4.1. While the magnitude of the EAL of the different structural typologies is a very useful decision making metric in PBEE, the values in Fig. 11 should be treated with care since these are case study structures with an estimated damageable inventory and an assumed seismicity. Nevertheless, the values presented here were of particular use to examine the relative trends and comparative differences in EAL for some of the different modelling assumptions outlined in Sect. 2, in addition to how one could identify the prominent sources of expected losses from disaggregation plots.

5 Retrofit of case study structures

Following the assessment of the various structure typologies, retrofit may be required to comply with legislation or the building owner's requirements in terms of expected performance, which could be ensuring life safety during more rare earthquake events or mitigating potential monetary losses from excessive damage during more frequent events. Examining the collapse assessment in Sect. 4.1, most structures considered here met, or were quite close to, the collapse criteria such that collapse was not established to be a significant issue that needed to be addressed via intervention in most cases, with the exception of the two-storey pilotis frame located in L'Aquila, for example. On the other hand, Sect. 4.3 examined the time-based loss assessment and reported the EAL for the different structure typologies examined.

Until recently, no requirements regarding acceptable levels of EAL were available in design codes or guidelines in Italy, meaning that its evaluation and subsequent decision-making rested entirely with the client. However, the Italian Ministry of Infrastructure and Public Works has recently introduced a seismic risk classification scheme (D.M. 58/2017) (Decreto Ministeriale 2017) that utilises the EAL of a building; in combination with another structural life safety index, to rank its seismic performance as initially proposed by Calvi et al. (2014). It is intentionally set up to be fully integrated with the Italian National Code (NTC 2008) so as to be more accessible to practising engineers. This framework therefore allows practitioners to evaluate the EAL of a building with relative ease; albeit through a number of simplifying assumptions to the original PEER PBEE framework utilised in this current study. In addition, a number of fundamental differences exist with some of the assumptions made in these guidelines with respect to the current study. For

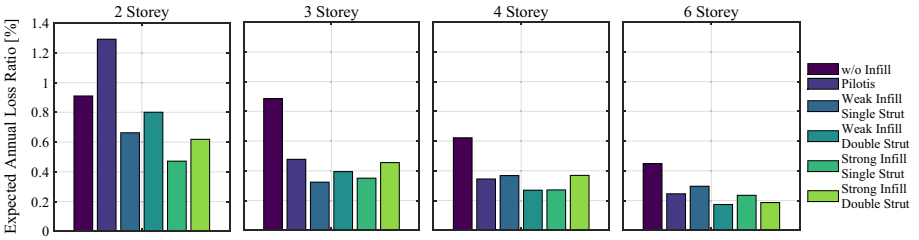

Fig. 11 EAL for each of the existing case study structures considered

example, one of the most significant ones is regarding the assumed replacement cost of the structure, which was reported by Cosenza et al. (2017) to have been assumed to be €1200 per m^2, whereas the current study was conducted using €1805.75 per m^2 meaning that the EAL values reported in Sect. 4.3 could be expected to be approximately 50% higher had this replacement cost been adopted. This aspect in addition to others related to the D.M. 58/2017 guidelines will be discussed in further detail in Sect. 6. For what concerns the decision to retrofit the case study structures examined here, it was assumed that improved performance vis-à-vis reduction in the EAL was required.

Retrofitting has traditionally implied that the structural elements be modified or upgraded to improve strength, stiffness or ductility capacity. Elnashai and Pinho (1998), among others, discuss different selective techniques with which these three aforementioned capacities of RC walls can be improved. Such retrofitting is defined in Eurocode 8 (EN 1998-1:2004 2004) in terms of the storey drift at the "damage limitation" limit state and the strength and ductility requirements and the "no-collapse" limit state. By controlling these two limit states, Eurocode 8 aims to provide adequate overall performance of the structure by both preventing structural collapse during rarer events and excessive damage during more frequent events. Similarly, NTC 2008, which is largely based on the specifications of the Eurocode, specifies the satisfaction of both the SLU and SLE limit states, which denote the ultimate and the serviceability limit states, respectively.

In light of the results in Sect. 4, this section examines the impacts of using a retrofitting philosophy, such as that outlined in NTC 2008 that would be typically adopted by practitioners, on the overall performance of the structure defined in terms of expected losses in addition to life safety of the structure. Section 5.1 first describes the different structural retrofitting solutions explored for the structures, where the sizing of such retrofits was in order to meet the requirements of NTC 2008 for both the serviceability and life safety limit states. The loss estimation procedure described in the previous section was then repeated and a comparison of the expected losses between the original frames and the structurally retrofitted frames is presented. Following this, non-structural element retrofit solutions were explored in Sect. 5.2 to examine the potential benefits of targeting selected non-structural elements in order to achieve the maximum impact in terms of reducing the expected monetary loss.

5.1 Structural retrofitting

In order to meet the requirements of NTC 2008, both the serviceability and ultimate limit states needed to be satisfied. The ultimate limit state requirements are defined to maintain a stable, ductile mechanism that avoids soft-storey failure through an appropriate strength hierarchy requirements. The serviceability limit state, on the other hand, defines the performance requirements in terms of the PSD to avoid excessive damage to the non-structural elements. This section describes the implementation of two retrofitting solutions to the case study structures: (1) RC jacketing of the column and beam-column joints and (2) the insertion of an RC wall.

For both retrofit solutions, it was assumed that the masonry infills were retrofitted by means of a perimeter gap between the infill and the surrounding RC frame in order to isolate the infill and prevent it from impeding the response of the RC frame. The provision of such a perimeter gap should indeed be large enough to accommodate large drift levels in the structure through the provision of elastic deformable materials in order to prevent damage to the masonry infills. A gap of up to 100 mm at the perimeter of the masonry infill could be expected accommodate up to 4% storey drift in the structures after which point

the structure will begin to engage the masonry infill. Using this retrofitting approach, it can be argued that it results in the situation where each of the case study frames behaves as a bare frame. Therefore, for simplicity in analysis, the frames previously modelled without infills were adopted in all cases and are retrofitted using the two aforementioned approaches. Given that such a large gap starts to become impractical, the ideal solution would be to modify the masonry infill models by inserting additional gap elements that can allow a certain amount of drift in the structure before being engaged in the structural response. However, citing the aforementioned study by Rossetto and Elnashai (2003), beyond a drift of 2.8–4.36% the structure is expected to start collapsing. Including the modelling of the perimeter gap may have provided additional lateral resistance at the higher intensities which would in turn increase the overall collapse capacity slightly. However, since these higher intensities would correspond to very higher levels of return period, the overall impact of this simplification on the EAL is anticipated to be very limited. Furthermore, the collapse performance may indeed be improved but was identified in Sect. 4.1 to not be a critical issue for the case study structures examined here. The masses at each level of the models was assumed to be constant in all cases, however. The RC jacketing of the columns and joints was intended to induce a beam-sway mechanism and avoid a soft-storey by ensuring the strength hierarchy at each joint satisfies the strong column-weak beam requirements of NTC 2008. The insertion of an RC wall also meant that a soft storey mechanism can be avoided and a more stable mechanism would be ensured. As noted by Charleson (2008), however, cutting a perimeter gap around the masonry infill will reduce the out of plane (OOP) stability of the infill as it becomes free on three edges and restrained on only one. This can be rectified by the provision of OOP restraints such as perimeter clips so that the overall OOP vulnerability of the frame can be assumed to be unchanged with respect to the original.

The RC jacketing was sized so that the strength hierarchy was maintained in accordance with the ultimate limit state requirements of NTC 2008. As such, no direct design calculations with respect to a design seismic hazard were required and that the required moment capacities for the column and joints were determined from the comparison of the beam moment capacities and the strength hierarchy requirements of NTC 2008. From this, it was assumed that an RC jacketing solution to achieve this capacity was provided to ensure a beam-sway as opposed to a potential non-ductile column-sway mechanism. In terms of numerical modelling, this was then represented by taking the required moment capacity of each column member and computing its yield curvature using the expression provided in Priestley et al. (2007) to give the effective stiffness of the retrofitted member. This increased effective stiffness and moment capacity were then used to model the behaviour of the columns with RC jacketing in a relatively simple manner since they have been sized using capacity design with respect to the beam capacities, whereas the beams were assumed to maintain the same behaviour as the original frame. For the RC wall retrofit, in order to maintain some level of consistency with the RC jacketing solution, a single RC wall of length 5 m, with thickness 250 mm was provided to each frame, where the moment capacity of the wall is set such that the total base shear capacity of the structure is approximately equal to that of the RC jacketing solution. Presuming that adequate foundations can be provided, an RC wall may be placed either at the exterior of the case study frames; provided it is effectively connected to the rest of the structure, or at the interior of a building so long as the architectural function of the building is not impeded. Furthermore, Fardis (2017) recently discussed how the upcoming revision of Eurocode 8 will incorporate a technique whereby entire bays of RC frames are filled in at each floor to transform them into essentially an RC wall retrofitted structure along the

height. Therefore, this retrofit may also be achieved by infilling one of the longer bays of the case study frames examined here but as previously stated, the actual layout of such interventions in practice ought to consider the architectural factors unique to each building. This was then represented numerically by adding a cantilever wall element with the required base moment capacity within each frame, as illustrated in Fig. 12, where the hysteretic backbone parameters in terms of strength and stiffness degradation are estimated using the expressions provided in Haselton et al. (2008) for ductile, well-detailed members. These retrofits resulted in a base shear increase of between 30 and 60% with respect to the frames modelled without masonry infill, where the larger increase was for the shorter structures.

This preliminary sizing of both retrofits was checked against the aforementioned code requirements at the serviceability and ultimate limit states. To do this, a design spectrum was required for the two limit states to check, using the N2 non-linear static procedure (Fajfar 2000), the respective requirements that were assumed to correspond to design return periods of 50 and 475 years for the serviceability and ultimate limit states prescriptions outlined in NTC 2008, respectively. The design spectra were constructed using the recommendation of the NTC 2008 and the PGA values required to construct the spectra were taken from the 2007 INGV hazard data available online (Montaldo and Meletti 2007). The site was taken to be located in Napoli as per Sect. 4.1, which has a PGA corresponding to 0.06 and 0.175 g for the two limit states considered. The code verification checks were taken to be that: (1) the maximum storey drift does not exceed 0.5% for damage limitation, as per NTC 2008, and (2) a stable mechanism results for no-collapse such that no soft storey mechanism is expected to develop. For the RC wall, this was done by adopting the expression provided in NTC 2008 for the ultimate chord rotation of the expected hinge location at the base of the wall. For the RC jacketing retrofit, the ultimate chord rotation capacity of the beam members was computed using a similar expression but with the modifications proposed by Melo et al. (2015) to account for the effects of the non-ductile detailing and use of smooth reinforcing bars on the ultimate chord rotation of the beam members. Following this approach, the drift profiles at the performance points are plotted in Fig. 13, where the maximum storey drift was reduced below the 0.5% threshold

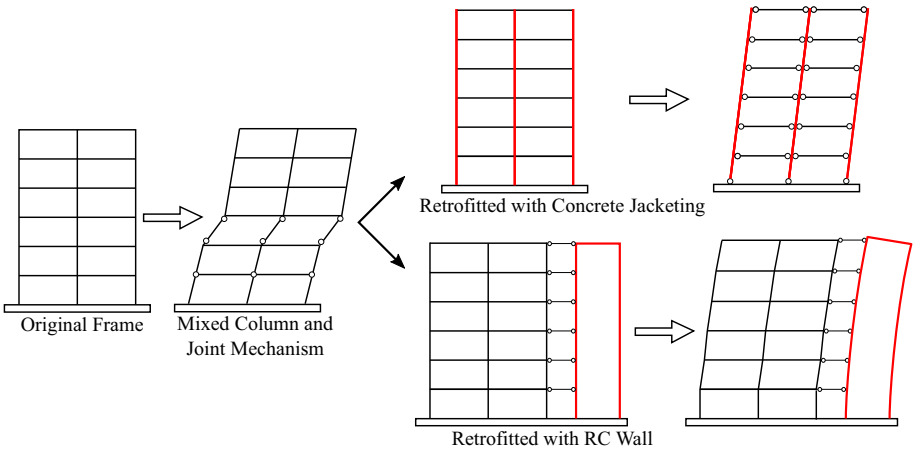

Fig. 12 Illustration of two different structural retrofitting strategies, which involved either the RC jacketing of the columns and joints or the insertion of an RC wall

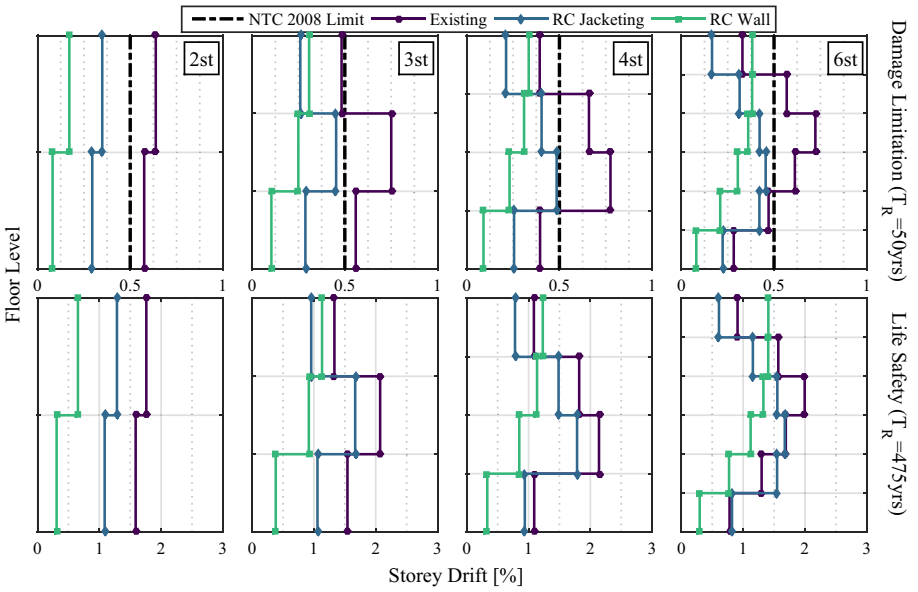

Fig. 13 Evaluation of the two structural retrofitting solutions with respect to the performance requirements at the two limit states considered

specified for the damage limitation in both retrofitting solutions. For the life safety limit state, the drift profiles were again reduced, which when combined with a beam-sway mechanism in the concrete jacketing retrofit and the RC wall ensured that a soft storey mechanism was avoided, results in the performance criteria being deemed to being satisfied. It was noted, however, that the RC wall retrofitting for the two and three storey frames were slightly conservative. This was a consequence of the simplistic assumptions to sizing the retrofit solutions adopted, whereas in practice one would expect to further refine and optimise such a retrofit design. Furthermore, cost–benefit analyses were not conducted for the individual retrofitting schemes and future work will look to incorporate this aspect along with some real archetype buildings to extend some of the conclusions drawn herein to these existing building cases also. These aspects are important as recent studies by Cardone et al. (2017a, b) who demonstrated that while certain types of retrofitting techniques may be rather effective, they may be unsustainable from an economical point of view when compared to other techniques.

For both of these structural retrofitting schemes outlined here, the NRHA was repeated using the retrofitted structural models to obtain the retrofitted response ordinates as a function of intensity that will be used to repeat the collapse and time-based assessment previously discussed. However, the list of damageable structural and non-structural elements needed to be updated since the performance of some elements, and therefore also the fragility functions and associated repair functions, were improved. The retrofitting carried out in each case consisted of either RC jacketing or insertion of an RC wall, in addition to the perimeter gap-cutting of any masonry infills. Table 3 shows the fragility functions that were used to assess the two retrofit cases.

Since the structural elements in the existing frame were upgraded via RC jacketing, a fragility function set was required to reflect the effect of concrete jacketing of the column and beam-column joints to ensure a beam-sway mechanism in the frames. Therefore, the

Table 3 Inventory list of the damageable structural elements with the corresponding assumed quantities, fragility and repair cost functions for each floor of the structural retrofitting

Retrofitting scheme	Damageable elements	Quantities	Fragility and repair cost functions
RC jacketing	Weak exterior beams	14	FEMA P58-3 (2012)—B1041.102a
	Weak interior beams	10	FEMA P58-3 (2012)—B1041.102b
RC wall	RC wall	32 m^2	FEMA P58-3 (2012)—B1044.003
	Non-ductile columns	12	Cardone (2016)—DWC (continuous)
	Exterior beam-column joints	14	Cardone (2016)—EWJs (end hooks)
	Interior beam column joints	10	Cardone (2016)—IWC

"Weak Exterior Beam" and "Weak Interior Beam" fragility functions were adopted from FEMA P58-3 (2012) as they represent weak beams with strong joints and a strong column-weak beam strength hierarchy. This was considered representative as the RC jacketing was expected to modify the structural behaviour in such a way that the columns and beam-column joints are no longer the weakest components and the beams were expected to form the mechanism, as reflected in the fragility functions adopted. In the case of the RC wall retrofitting scheme, the existing vulnerable elements such as weak columns and beam-column joints remained but the RC wall needed to be considered. As such, this was done using the fragility function listed for the RC wall in Table 3 adapted from FEMA P58-3 (2012). This was considered representative as the original frame was still vulnerable to the at the same locations, therefore the previous fragility function set remained, in addition to adopting the RC wall fragility function as this represented a new element in the structure that was expected to form plastic hinging at its base. This fragility function defines the damage to the RC wall as a function of storey drift, although more refined methods of assessment using the wall base hinge curvature, for example, would be anticipated to be a better demand parameter to estimate damage but was not the focus of the current study and the drift dependant fragility function was deemed appropriate for the comparative study discussed herein. Adopting this fragility function also assumes an RC wall section detailed to modern seismic detailing provisions.

5.2 Non-structural retrofitting

While the previous section looked to improve the overall performance by strengthening and stiffening the structures, this section examines some of non-structural retrofit solutions. This comes from the fact that a large percentage of the direct monetary losses in a structure arise from damage to the non-structural elements (Taghavi and Miranda 2003). Therefore, more prudent solutions when mitigating expected loss may be to reduce the vulnerability of elements contributing most to the losses. Compared to the case of structural retrofitting, non-structural retrofitting offers some benefits aside from those to be discussed in Sect. 5.3. Among these is the ease at which non-structural retrofits can be implemented with respect to structural retrofits. For example, to retrofit using RC jacketing, one needs to uncover each element in the structure that may be buried behind partition walls or other fixtures and fittings. Following this, extensive work to prepare the existing structural element and insert the additional reinforcement and concrete needs to take place, such that continued occupancy of the structure during retrofit is unlikely to be possible. On the

contrary, retrofit of an air-handling unit placed at the roof level, for example, may consist of inserting isolators beneath the units with relative ease. In addition, the insertion of additional piping bracing or ceiling system restraints can also be carried out relatively easily compared to a solution that requires a structure to remain unoccupied while structural modifications are being undertaken.

The idea of considering the non-structural elements in a structure as a retrofitting option to reduce the expected losses in a structure has been previously trialled in Calvi et al. (2014), where the option of improving internal partition details to reduce their vulnerability to drift demand in a ductile RC frames was outlined conceptually. It should be noted, however, that retrofit of non-structural elements will mainly target the expected losses and in cases where the probability of collapse is unacceptably high, it would not suffice as a means to satisfy both of the code requirements. As such, this idea of retrofitting non-structural elements inherently assumes that the collapse requirements were met, which were checked in Sect. 4.1. This section expands on this concept, whereby the expected losses in different structural typologies typical to GLD RC frames in Italy were examined, proposing ways in which the overall performance of these structures can be improved by considering alternative retrofitting strategies that target losses in both the drift and acceleration sensitive elements. Such an approach can be justified when considering that non-structural elements in existing buildings constructed in Italy prior to the 1970s are not likely to have any seismic provisions for adequate protection of non-structural elements, seeing as the first consideration of assessing forces on non-structural elements appeared in 1964 Uniform Building Code in the US (Filiatrault and Sullivan 2014). That is, the minimum requirements in terms of fixtures and fittings for the various non-structural elements are anticipated to have been installed such that the element remains in place, but no proper consideration given to its protection under seismic excitation. This was observed during the site visits to the school buildings throughout Italy (O'Reilly et al. 2017a, b, c) where, for example, the suspended ceiling system consisted of just vertical hangers to fix the ceiling to the underside of the upper slab, whereas no consideration was given to inserting diagonal splay wires to prevent excessive movement horizontally. Therefore, existing fragility functions for non-structural elements with no seismic design provisions can be considered adequate to estimate the damage of these elements examined here. The retrofitted non-structural elements, on the other hand, are evaluated with fragility functions designated for elements with seismic design provisions as the retrofitting scheme implemented was intended to bring the element's seismic performance in line with the modern design code requirements, such as ASCE 7-10 (ASCE 7-10 2010). Fragility functions for improved non-structural elements were taken from the FEMA P58-3 (2012) database and are listed in Table 4. This considers that the seismically deficient non-structural elements, initially assumed as part of the building's damageable inventory in Sect. 4.2.1, were retrofitted to bring them in line with current design code requirements. In contrast to the structural retrofit scenarios, no re-running of NRHA was required as the response of the structures was taken as independent of the non-structural components, meaning that the improved fragility functions were inserted in place of the older ones and the loss estimation analysis repeated.

5.3 Assessment of retrofitted structures

Using the different structural and non-structural retrofitting schemes outlined in the previous sections, this section examines the performance in terms of collapse and direct economic losses, as before. A number of different non-structural retrofitting schemes are

Table 4 Inventory list of the improved non-structural elements with the corresponding quantities, fragility and repair cost functions for each floor in the case of non-structural element retrofitting

Damageable elements	Quantities	Fragility and repair cost functions
Internal gypsum partitions (w/slip tracks)	100 ft	FEMA P58-3 (2012)—C1011.001d
Internal gypsum partition wallpaper finish (w/slip tracks)	100 ft	FEMA P58-3 (2012)—C3011.001d
Internal gypsum partition ceramic tile finish (w/slip tracks)	100 ft	FEMA P58-3 (2012)—C3011.002d
Suspended ceilings (additional lateral bracing)	1065 ft^2	FEMA P58-3 (2012)—C3032.003b
Cold water piping (additional bracing)	1000 ft	FEMA P58-3 (2012)—D2021.013a
Cold water piping bracing	1000 ft	FEMA P58-3 (2012)—D2021.013b
Hot water piping (additional bracing)	1000 ft	FEMA P58-3 (2012)—D2022.013a
Hot water piping bracing	1000 ft	FEMA P58-3 (2012)—D2022.013b
Glazed windows***	10	Sassun (2014)—Glazing Panels 1.0 × 2.5 m
Lighting (additional lateral bracing)	15	FEMA P58-3 (2012)—C3034.002
Elevator***	1*	FEMA P58-3 (2012)—D1014.012
HVAC in-line fan (additional lateral bracing)	2	FEMA P58-3 (2012)—D3041.002c
HVAC ducting (additional lateral bracing)	2	FEMA P58-3 (2012)—D3041.011c
HVAC diffusers (additional lateral bracing)	2	FEMA P58-3 (2012)—D3041.031c
HVAC fan	1**	FEMA P58-3 (2012)—D3041.101a
Chiller (vibration isolated)	1*	FEMA P58-3 (2012)—D3031.013a
Air handing unit (vibration isolated)	2**	FEMA P58-3 (2012)—D3031.023a

* At ground level only

** At roof level only

*** Not retrofitted

examined to highlight the impacts when targeting either drift or acceleration sensitive elements, or a combination of both in addition to the two structural retrofits. The retrofitting solutions to and labelling system adopted herein for each are listed here for clarity:

- Retrofit A—Improved detailing for both the drift and acceleration sensitive non-structural elements.
- Retrofit B—Improved detailing for the drift sensitive non-structural elements.
- Retrofit C—Improved detailing for the acceleration sensitive non-structural elements.
- Retrofit D—Structure retrofitted by RC jacketing the column and beam-column joints and masonry infill isolated from surrounding frame.
- Retrofit E—Structure retrofitted by inserting an RC wall and masonry infill isolated from surrounding frame.

It should be noted that the masonry infill was classified as a structural element, as initially indicated in Table 2, under the hypothesis that it significantly modified the structural behaviour of buildings. This means that retrofits A–C do not possess any modification to the influence of the masonry infill on frame behaviour and focused solely on the non-structural elements listed in both Tables 2 and 4, whereas the structural retrofits labelled D and C assumed the infill was sufficiently isolated from the surrounding through the provision of a sufficient gap to not impede the response of the structural retrofit

elements and not result in any non-ductile failure associated with interaction of the frame and masonry infill at limit states far from collapse.

5.3.1 Collapse assessment

The initial collapse assessment of the case study structures outlined in Sect. 4.1 indicated that the collapse safety of the structures was satisfactory when compared to limits proposed in current guidelines. However, in order to appreciate the effects that the structural retrofitting has on the collapse performance of the frames, the probability of collapse at the MCE level previously outlined in Sect. 4.1 was computed and shown in Fig. 14 for the retrofitted structures. Comparing the probabilities of collapse at the MCE intensity, it can be seen from Fig. 14 that the retrofitting of the non-structural elements had no impact on the collapse fragility of the structures, which was expected since the non-structural elements were not explicitly modelled in neither the existing nor the retrofitted structures, meaning that the collapse fragility remained unchanged. Likewise, the collapse performance of the structurally retrofitted structures was markedly improved.

5.3.2 Time-based loss assessment

By integrating these individual vulnerability functions determined for each of the retrofitting cases with the mean hazard curves, a time-based assessment was carried out to examine the impact of the different retrofitting strategies on the EAL. Figure 15 plots the EAL for each of the original structural typologies along with the EAL for each of the five retrofitting schemes investigated here. These were separated in terms of storey number and structural typology to illustrate the respective influence of the retrofitting in each case.

From the information presented in Fig. 15, a number of general observations can be made regarding the effectiveness of the various retrofitting strategies. The first observation is that the retrofitting of the non-structural elements was a beneficial solution in every case whereas depending on whether the structural typology was a frame modelled with or without infill, the drift or acceleration-based schemes have the greatest impact. For the case of the frames modelled without infills, a mean reduction in EAL of approximately 24% was noted for drift-based retrofitting whereas only a 12% reduction was observed for the acceleration-based retrofitting. Compare this to the case of the infilled frames, where PSD-based retrofitting reduced the EAL by approximately 10% whereas acceleration-based returned up to a 60% reduction, highlighting the apparent importance of acceleration sensitive elements in the overall performance of infilled frames. This is noteworthy as some traditional approaches to retrofit, such as those prescribed for the SLE limit states of NTC 2008, aim to mitigate excessive damage and maintain the structures operational function by limiting the drift in the structure.

6 Discussion and implication for PBEE

6.1 Implications of different retrofitting considerations on EAL

Examining the performance in terms of EAL of the structural retrofits with respect to the existing structures in the previous sections, some rather peculiar results were observed at first. While some results show how both RC jacketing and inserting an RC wall reduces the

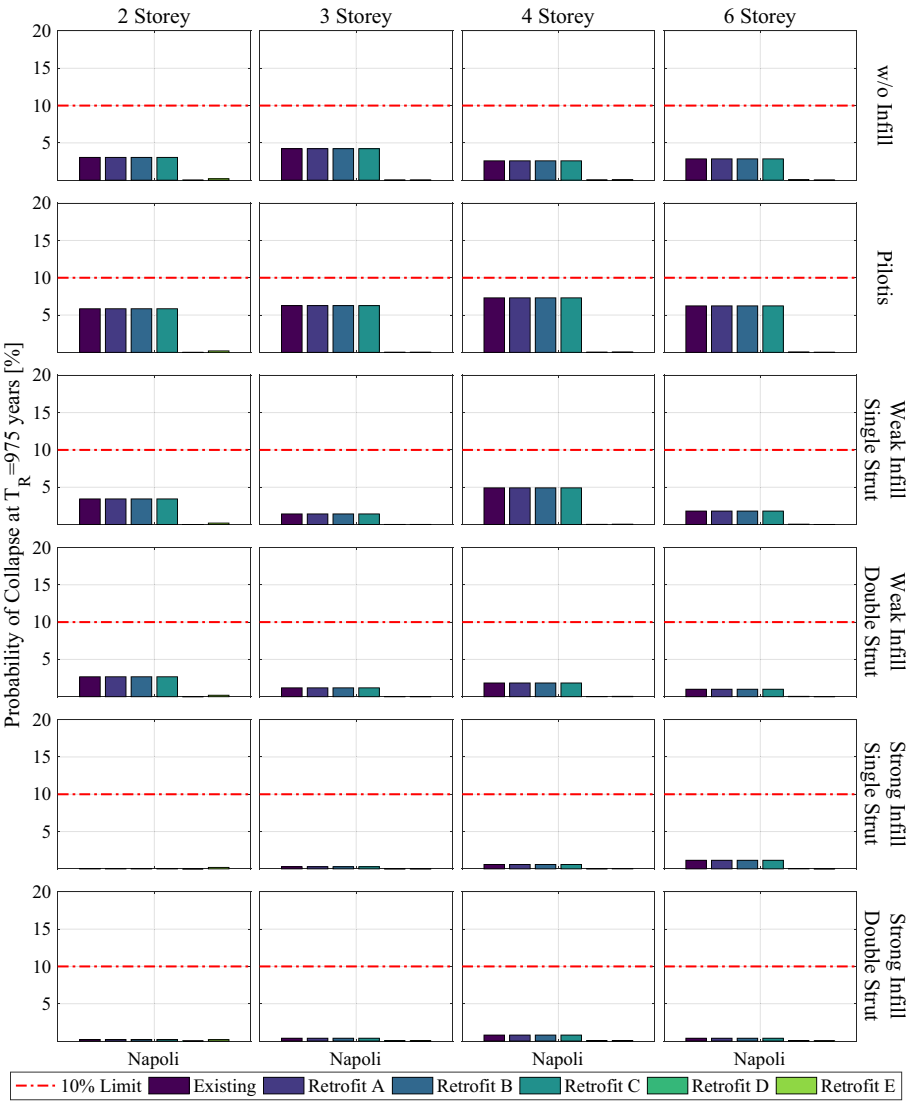

Fig. 14 Probability of collapse for the different retrofitted case study structures that is checked at TR = 975 years to not exceed a value of 10%, as per the FEMA P695 (2009) guidelines

EAL, some instances arose where this EAL was actually worsened (i.e. increased), with Fig. 16 illustrating two specific cases. Examining the performance of these, some questions arise as to why this occurred if both were intended to improve performance by satisfying the prescribed drift limits. It was noted that in both cases, the probability of collapse of the retrofitted frames decreases significantly (Fig. 14), although Fig. 16 illustrates that despite this improvement, the subsequent change in expected loss due to increased floor acceleration and/or more distributed damage throughout the height of the structures has worsened the performance of the entire buildings defined in terms of EAL. This raises the issue that when initially assessing the structures in Sect. 4.1, the collapse assessment of these

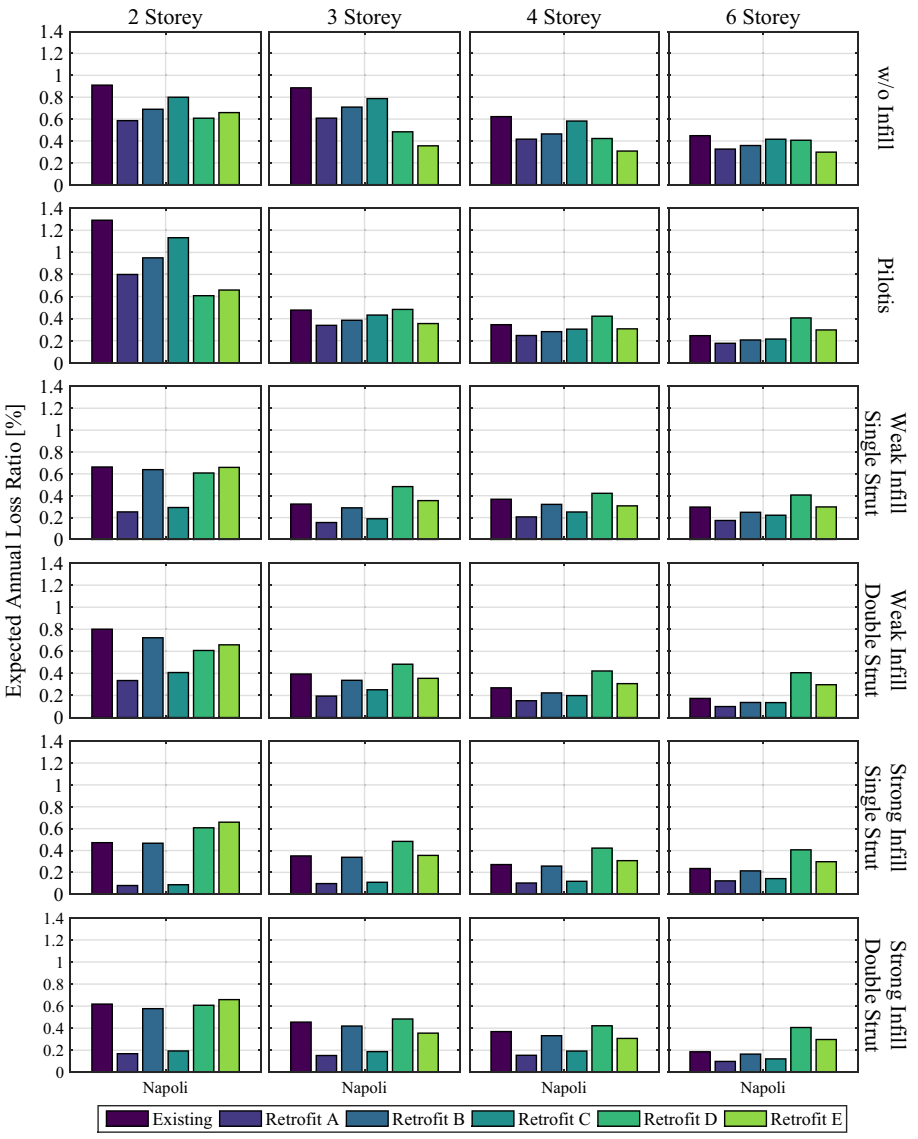

Fig. 15 EAL for each of the structural typologies along with the retrofitting schemes described to show the relative impact of each with respect to the existing structure

particular structures was shown to meet the prescribed criteria. The EAL of these structures were deemed to have not been satisfactory and the code prescriptions to retrofit the structure in order to meet the prescribed drift limits at the damage limitation being implemented in Sect. 5.1. Figure 16 illustrates that this initial objective of improving the performance of the structure in terms of EAL has, in fact, been worsened meaning that the result was a structure more resilient to collapse but more susceptible to monetary losses, despite collapse not being the issue at hand in the first place. It should be noted, however, that some cases, such as the two-storey strong infilled frame modelled with single struts

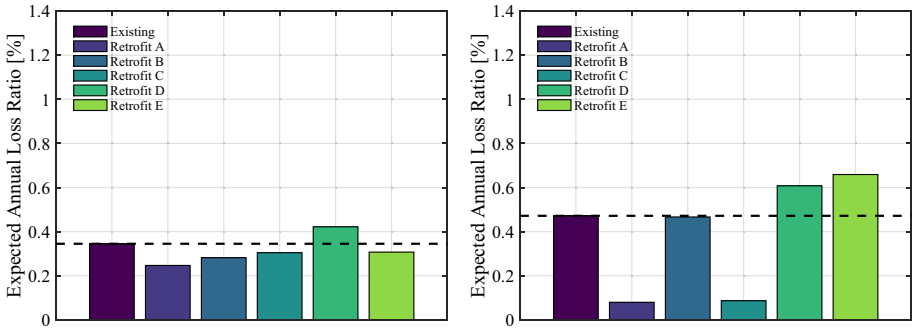

Fig. 16 Illustration of the effectiveness of the different retrofitting strategies gauged in terms of EAL for the case of the four-storey pilotis frame (left) and two-storey strong infill frame modelled with single struts (right)

Fig. 17 Illustration of the relative improvement in performance defined in terms of EAL with respect to the existing structure. Points above the 1 to 1 line correspond to cases where the EAL of the structure actually increased following the retrofitting measure

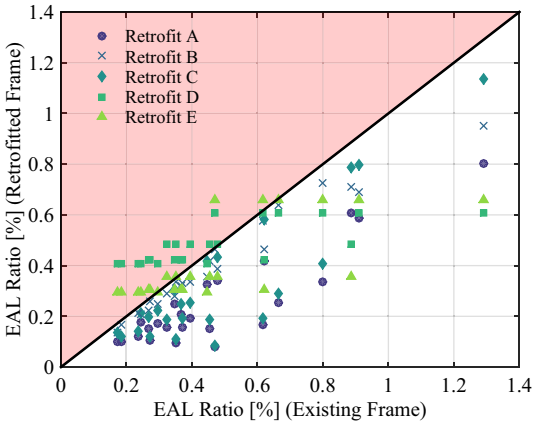

shown in Fig. 16, exhibit a decrease in the EAL for the case of RC jacketing, albeit rather small, which was more in line with the initial objective of retrofitting the structure.

These cases where the structural retrofitting of the structures actually worsened the performance in terms of losses are illustrated in Fig. 17, where a plot of the EAL before versus after retrofitting using the different techniques previously described is shown. Points above the one-to-one line correspond to these cases where the retrofitting measure worsened the structure's performance defined in terms of EAL. This was a rather strange observation at first, as one would expect the performance of the structure to be improved following structural intervention, so the question remains as to why this occurs? As previously mentioned, the EAL is the integration of the vulnerability function with the mean hazard curve and so a reduction in vulnerability ought to correspond to a reduction in EAL. However, this assumes that the mean hazard curve has also remained unchanged in addition to a uniform improvement of the vulnerability curve at all intensities with respect to the original.

Figure 18 illustrates this remark more clearly, to which there are actually two observations to make. Structural retrofitting illustrated as a strengthening and stiffening of the structure in Fig. 18a, therefore, appears to become a trade-off where the expected demand

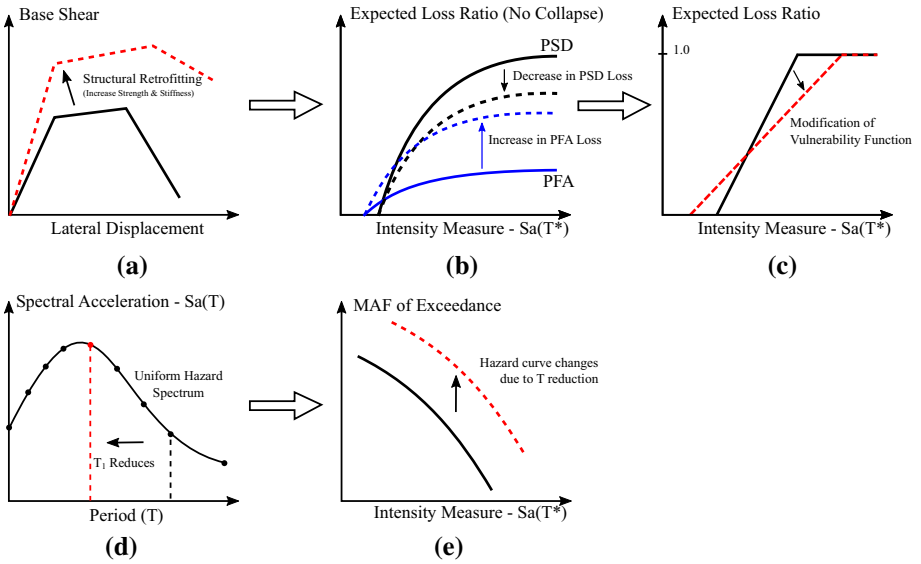

Fig. 18 Illustration of the potential impact of structural retrofitting where strengthening and stiffening of the structure can actually worsen the EAL performance due to the combined effect of an increase in loss from higher PFA and a shift in the mean hazard curve due to period shortening. **a** Assessment of existing building, **b** demand parameter disaggregation, **c** loss estimation of building, **d** impacts on spectral values, **e** hazard modification

decreases in one source possibly resulting in an increase in the other, as illustrated in Fig. 18b. This is also combined with the fact that the new prominent source of losses may actually be occurring at a lower, more frequent intensity level to further increase the weighting during the hazard integration, which is shown in Fig. 18c through the decrease in the intensity required to begin accumulating expected losses. This aspect was observed during the recent 2016 earthquake in Ecuador for hospital buildings, where Morales et al. (2017) noted how following the 1998 earthquake in Ecuador, the Ecuadorian Ministry of Public Health embarked on a programme to retrofit existing hospital structures by strengthening through RC jacketing and RC walls to a level far beyond the building code requirements and achieve an almost elastic building response. Morales et al. (2017) noted how this approach would be expected to lead to higher PFA in the structures and subsequently increase acceleration-sensitive damage. Following the 2016 earthquake, post-earthquake reconnaissance of the hospital buildings by O'Connor and Morales (2016) reported that although none of the hospital facilities collapsed, 22 were left inoperative due to excessive non-structural damage. This resulted in aid being provided from temporary shelters, which resulted in overcrowding and unsanitary conditions. The observation of these counterproductive strengthening measures carried out in Ecuador echo the above comments regarding the potential worsening of performance due to excessive structural retrofitting when more prudent solutions to improve the overall building performance may be available. The recent findings of Cardone et al. (2017a, b) also echo the above observations where the strengthening and stiffening of the masonry infill panels using techniques such as fibre reinforcing polymers were observed to be unsustainable from an economical point of view when compared to other techniques such as base isolation. This was due to their ineffectiveness in reducing the EAL of the case study buildings to a significant degree

compared to the initial cost of retrofitting. While Cardone et al. (2017a, b) did not explore this ineffectiveness of this retrofitting technique in further detail, it is envisaged that the above remarks regarding the trade-off in drift and acceleration sensitive losses when strengthening and stiffening the structures played a significant role.

The second aspect of the structural retrofitting highlighted here and illustrated in Fig. 18d is the modification of the fundamental period of vibration of the structure (T_1) as result of the strengthening and stiffening. This results in a change in T_1 which, when combined with the IM employed here of $Sa(T_1)$, means that the definition of the mean hazard curve must also be updated to maintain consistency in the definition of IM. For example, the structural retrofits examined in Sect. 5.1 exhibited average period reduction of 38 and 142% were observed for the RC jacketing and insertion of RC walls, respectively. In cases like those illustrated in Fig. 18d, this will result in an increase in the mean annual frequency (MAF) of exceedance for a given level of intensity, resulting in an increased EAL. These two observations regarding structural retrofitting help explain the cases shown in Fig. 15 in which the strengthening of the structure actually worsened the performance when defined in terms of EAL. It should be noted that while the general theme of the discussion presented above indicates that engineers should instead focus on non-structural elements when retrofitting a structure, it is maintained that the fundamental requirement of ensuring life safety still needs to be satisfied. In addition, considering the assumptions made in Sect. 3.2 with regards to the hazard compatibility of the ground motion record set used, the results presented here should be treated in a comparative rather than an absolute manner taken to be representative values of EAL for existing GLD RC frames with masonry infill. Furthermore, an exhaustive study of the different non-structural elements specific to different types of Italian occupancy was not considered in detail, although every effort was made to ensure the information was reasonably representative based on surveys of existing buildings in Italy. The above discussion is intended to give the reader the sense that while the work presented here offers insight into relative impacts of different retrofitting strategies, it is only a comparative study for the case of GLD RC frames in Italy.

6.2 Role of EAL within a seismic performance classification framework

Some additional aspects to be considered for the use of EAL as a standardised performance measure following the PEER PBEE framework, as initially proposed by Calvi et al. (2014), are illustrated in Fig. 19. One of the first issues illustrated in Fig. 19 for the computation of EAL is related to the collapse probability, P[C|IM]. In order to have a suitable assessment of collapse fragility, all of the failure modes contributing to the collapse of the structure should be accounted for. For example, previous research by Ibarra et al. (2005) highlighted the need to consider the post-peak strength degradation in addition to the inclusion of P-Delta effects for collapse. In addition to this, Sect. 3.3 has shown the importance of considering the shear failure in the column members due to the interaction with the masonry infills, where a reduction of up to 10% in the median collapse intensity was observed and an overall increase in the probability of collapse. As such, the inclusion of all potential failure modes is vital to the appropriate representation of the collapse vulnerability in loss estimation. A second issue is the appropriate computation of a replacement cost value since the EAL ratios plotted in Fig. 17 are expressed as a percentage of the replacement cost of the entire structure. Therefore, if a building owner were to assess their building in terms of the seismic performance classification framework outlined in Calvi et al. (2014) and find that their building fell just outside of the acceptable performance

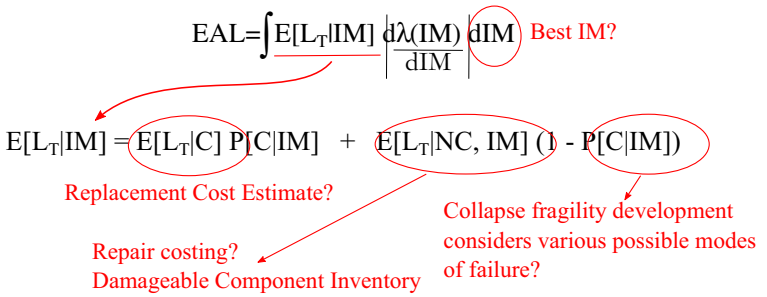

Fig. 19 Various considerations when using EAL as a seismic performance classification metric

class range meaning intervention was required to improve its performance, the temptation would exist on the building owner's behalf to slightly overestimate the buildings replacement cost to artificially reduce the EAL ratio and fall within the acceptable range to result in no required intervention. As such, proper guidance on replacement cost estimation would be required when adopting the PEER PBEE methodology to avoid such situations but still take into account the variation in replacement costs with respect to structural typology and differences in regional pricing throughout Italy. Thirdly, the compilation of a representative list of damageable elements and appropriate repair costs should be prescribed in order to achieve the same answer regardless of who applies the process, thus avoiding situations such as that highlighted in Calvi et al. (2014) where for the same case study RC frame structure examined in the US, two independent studies (Krawinkler 2005; Porter et al. 2004) to quantify the EAL resulted in a difference of over three times when different assumptions regarding replacement costs and damageable inventory were made. These aspects are ones in which clear instruction in the form of guidelines can ensure more congruent results, or the adoption of ready-made demand-to loss-functions, such as those outlined in Ramirez and Miranda (2009), for example, that are defined based on the building occupancy type. Last is regarding the use of an appropriate IM, where $Sa(T_1)$ is employed in this study as it is adopted in numerous studies and guidelines, such as FEMA P58 (2012a, b). However, more recent research by Kohrangi et al. (2016), among others, suggest that more advanced IMs may actually provide a better way with which to represent the intensity, as opposed to $Sa(T_1)$. Future research may investigate the incorporation of more advanced IMs that are less dependent on T_1 so as to reduce the impact of modifying the modal properties of the structure on the computation of annualised losses, among other issues related to IM choice. The interested reader is referred to recent work by Kazantzi and Vamvatsikos (2015) and Kohrangi et al. (2017), among others, for some potential candidates.

The above remarks on the implementation of a seismic performance classification guideline in Italy utilising EAL as a performance measure have very recently been realised in Italy through the D.M. 58/2017 document issued by the Italian Ministry of Infrastructure and Public Works (Decreto Ministeriale 2017). As briefly mentioned in Sect. 5.1, these guidelines are intentionally set up to be fully integrated with the Italian National Code and to be more accessible to practitioners. From the above discussion, this clearly represents a step in the right direction for increased seismic resilience. As discussed in Calvi et al. (2014) and Porter et al. (2004), framing the discussion of assessment and retrofitting of buildings in terms of not just life safety, but also monetary loss metrics such as EAL, will not only result in more resilient communities that can cope with the induced damage of an

earthquake but also serve as a means with which a building's seismic resilience can be incorporated into a cash-flow analysis and determining insurance premiums, for example.

Since these guidelines, whose methodology is summarised Fig. 20, are intended to be implemented rather quickly, a number of simplifying assumptions have been made to indirectly mitigate many of the issues raised previously when implementing the PEER PBEE methodology in Fig. 19. Instead of requiring the users to conduct extensive numerical analyses on detailed models to characterise structural response and develop damageable component inventories with which to compute economic losses, the guidelines simply require the user to perform a pushover analysis of the structure and determine the annual rate of exceeding the different limit states using code-defined procedures. By assigning a loss ratio to each of these limit states, the EAL is simply computed as the are under curve, similar to what was conducted by Welch et al. (2014), for example. In doing so, many of the above considerations in Fig. 19 have been removed from the user's control. For example, Fig. 20f outlines how each limit state in the building is directly assigned an expected loss ratio, whose determination is discussed a little further in Cosenza et al. (2017). These authors described how these expected loss ratios were determined for the SLD and SLV limit states by considering the actual losses reported by Dolce and Manfredi (2015) following the 2009 L'Aquila earthquake in Italy. This process assumed that these SLD and SLV limit states corresponded to the B/C and E classifications of the AEDES evaluation form (Dipartimento della Protezione Civile 2013) used by the Italian Department of Civil Protection following the earthquake. By using the repair costs associated with each building examined, the mean value was found and by assuming the replacement cost to be €1200 per m^2, ratios of 15 and 50% were established for SLD and SLV, respectively, as illustrated in Fig. 20f. The other limit states SLO and SLC were simply defined as 7.5%; corresponding to half of SLD, and 80%, respectively. While this approach is good since it utilises real data from a recent earthquake in Italy, it makes no distinction between building usage and function, which may play an important part in the repair costs.

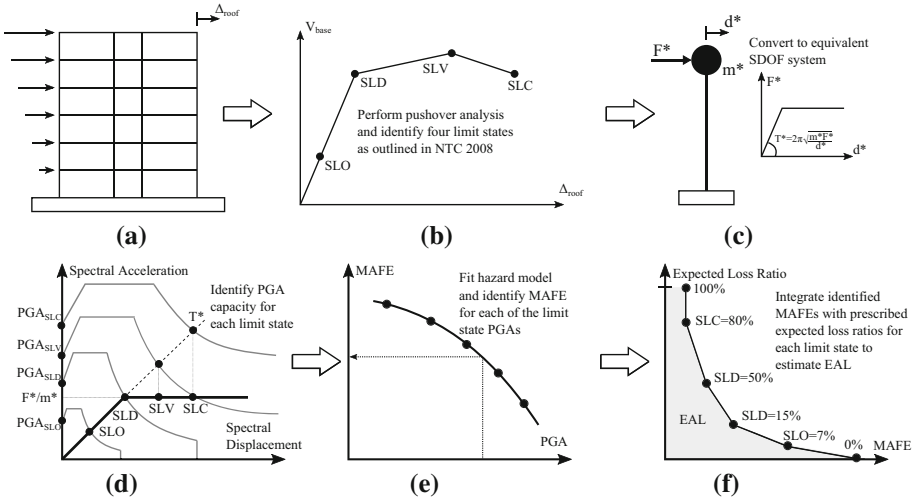

Fig. 20 Fundamental steps involved in computing the EAL using the D.M. 58/2017 seismic performance classification guidelines issued by the Italian Ministry of Infrastructure and Public Works (Decreto Ministeriale 2017). **a** Static pushover analysis, **b** identification of limit states, **c** conversion to equivalent system, **d** identify PGA of LSs, **e** identify MAFE of LSs, **f** compute EAL

It also, and more critically, relieves a number of decisions from the practitioners that were identified in Fig. 19. However, while this may be favourable for a simplified approach, a number of these assumptions may require further scrutiny. The most important of these comes in relating specific code-defined limit states with visual interpretations of damage following an earthquake, which are subject to the surveyor's judgement, may be highly variable and most likely conservative. Compared to the PEER PBEE methodology, where detailed numerical analysis is conducted and the evolution of damage and subsequently economic losses are tracked in a more consistent way; albeit with a number of important input variables to be decided by the user outlined in Fig. 19, the simplified methodology of Fig. 20 introduces a deal of uncertainty that is beyond the control of the analyst.

Furthermore, the classification scale introduced in these new guidelines has a number of limitations, where depending on the EAL compute in Fig. 20 a letter-based score ranging from A + through to G, with A + being the most desirable score, is assigned. As initially discussed in Calvi et al. (2014), this ranking system presents a metric with which increased seismic resilience can be quantified and demonstrated in more meaningful terms. However, Cosenza et al. (2017) discuss the process with which these different classification ranks were established, where the theoretical limits of 0–10% for the EAL of a building were established and the classification scheme defined as eight different limits within these bounds. No detailed studies using the rigorous PEER PBEE approach were conducted to quantify appropriate limits and in the opinions of the authors, ought to be refined further in future studies since there is no data; analytical nor empirical, to suggest whether a mid-rank rating of D for example ($2.5\% < \text{EAL} \leq 3.5\%$) is actually realistic. Analytical studies on Italian construction typologies to date suggest that it is not, with studies such as Cardone and Perrone (2017) reporting values of 0.75–1.42% for building typologies similar to those considered here, which are similar to the values reported Fig. 11 in the current study when taking the higher replacement cost adopted here. Furthermore, when discussing the idea of such a classification scheme, Calvi et al. (2014) collected the available results for the EAL of a number of case study buildings examined in the US and used this as a basis for some tentative ranking bounds. An average value of 2.5% EAL was identified for non-ductile RC frame buildings in California, which when considering the higher seismicity of that region with respect to Italy, it appears that the D rating tier mentioned above seems somewhat unrealistic. This represents some of the aspects that future work should strive to address such that consistent and univocal values of EAL can be computed either from the simplified methodology outlined in Fig. 20 or from the more refined and extensive PEER PBEE methodology. Such future work should look to conduct large parametric studies on a number of building typologies to quantify appropriate ranges in order to further refine the definitions of performance. Furthermore, aspects such as building usability should also be incorporated in some way as work by Ramirez and Miranda (2009), for example, have highlighted the difference in expected monetary losses depending on the building usage.

7 Summary and conclusions

The various aspects discussed in this article have been aimed at provide further insight at the application of the PEER PBEE loss estimation methodology to existing GLD RC frames with masonry infill. This was exhibited through the detailed analysis of various typologies in Sect. 3, followed by the application of the methodology from a practitioner's

point of view in Sect. 4 and the subsequent retrofitting of these structures following traditional code-oriented approaches. Some implications of the approach were discussed collectively in Sect. 6 to provide discussion on the current state-of-the-art application of this methodology to GLD RC frames with masonry infill, in addition to offering some insight to practitioners on the implications of different aspects of the assessment methodology, including the recent seismic performance classification framework guidelines in Italy, and also the recent seismic performance classification framework guidelines in Italy. The main findings of this article are:

- Modelling of the shear behaviour of the column members to capture the effects of shear damage due to interaction with the masonry infill on the response was shown to increase the first mode period by up to 12%. It was also shown how the failure of the columns in shear for the strong infill cases resulted in a reduced base shear capacity of the frame along with a reduced overall lateral drift capacity. This impact of the direct shear hinge modelling was also noted during the collapse assessment where, generally speaking, the inclusion of a double strut infill model with shear hinges in the columns resulted in a decrease of up to 10% in the median collapse intensity. Despite this increased flexibility, the modelling of the infilled frames with column shear behaviour resulted in both a general increase in EAL and collapse probability, highlighting the importance that such a behaviour be included in the assessment of GLD RC frames with masonry infill.
- Retrofitting of the non-structural elements can have a comparative, if not better impact on the EAL than that of structural retrofitting provided that the collapse prevention requirements are met. This aspect implied that, should the collapse performance of a structure be sufficiently low but the overall performance of the structure in terms of monetary losses be unacceptably high, it may be more beneficial to consider the retrofitting of the main culprits contributing to the expected loss, that are in this case the non-structural elements, rather than applying strengthening and stiffening measures that may actually worsen the situation when speaking in terms of EAL.
- In some cases, the strengthening and stiffening of the structure by inserting additional structural elements were seen to worsen the performance of the structure when defined in terms of EAL. This resulted as a combination of the trade-off in the reduction of drift-induced damage with the increase in acceleration-induced damage; in addition to the change of the definition of hazard due to the periods shortening of the structure as a result of the IM employed. This should be noted as it clearly illustrated that strengthening and stiffening are not necessarily a beneficial when speaking in terms of direct monetary losses.
- Comparing the recently proposed seismic performance classification framework in Italy with some of the points of discussion raised in relation to the PEER PBEE methodology, it was seen how many of the concerns raised here in relation to the robust and replicable implementation of the extensive methodology have been indirectly addressed by the new classification framework. It was seen how these were addressed through the need to simplify the overall methodology and integrate it with existing code assessment procedures. While it was acknowledged that the introduction is a positive step in the field, there are still a number of aspects that should be addressed as part of future studies.

Acknowledgements The authors would like to acknowledge the funding provided by the ReLUIS consortium and the first author acknowledges the funding provided by the IUSS Pavia doctoral programme. The

constructive comments of two anonymous reviewers helped improve the overall quality of this paper. In addition, the assistance provided by Matteo Moratti in estimating repair costing for Italy is also gratefully acknowledged.

References

ASCE 7–10 (2010) Minimum design loads for buildings and other structures. ASCE 7–10, Reston
Baker JW (2015) Efficient analytical fragility function fitting using dynamic structural analysis. Earthq Spectra 31(1):579–599. https://doi.org/10.1193/021113eqs025m
Baker JW, Lee C (2017) An improved algorithm for selecting ground motions to match a conditional spectrum. J Earthq Eng. https://doi.org/10.1080/13632469.2016.1264334
Calvi GM, Sullivan TJ, Welch DP (2014) A seismic performance classification framework to provide increased seismic resilience. In: 2nd European conference on earthquake engineering and seismology, Istanbul, Turkey
Cardone D (2016) Fragility curves and loss functions for RC structural components with smooth rebars. Earthq Struct 10(5):1181–1212. https://doi.org/10.12989/eas.2016.10.5.1181
Cardone D, Flora A (2017) Multiple inelastic mechanisms analysis (MIMA): a simplified method for the estimation of the seismic response of RC frame buildings. Eng Struct 145:368–380. https://doi.org/10.1016/j.engstruct.2017.05.026
Cardone D, Perrone G (2015) Developing fragility curves and loss functions for masonry infill walls. Earthq Struct 9(1):257–279. https://doi.org/10.12989/eas.2015.9.1.257
Cardone D, Perrone G (2017) Damage and loss assessment of pre-70 RC frame buildings with FEMA P-58. J Earthq Eng 21(1):23–61. https://doi.org/10.1080/13632469.2016.1149893
Cardone D, Gesualdi G, Perrone G (2017a) Cost-benefit analysis of alternative retrofit strategies for RC frame buildings. J Earthq Eng. https://doi.org/10.1080/13632469.2017.1323041
Cardone D, Sullivan T, Gesualdi G, Perrone G (2017b) Simplified estimation of the expected annual loss of reinforced concrete buildings. Earthq Eng Struct Dyn. https://doi.org/10.1002/eqe.2893
Charleson A (2008) Seismic design for architects—outwitting the quake. Elsevier Ltd, Oxford
Cornell CA, Krawinkler H (2000) Progress and challenges in seismic performance assessment. PEER Cent News 3(2):1–2
Cosenza E, Prota A, Di Ludovico M, Del Vecchio C (2017) Il metodo convenzionale per classificare il rischio sismico delle costruzioni. Costruire in Laterizio 171:70–77
Crisafulli FJ, Carr AJ, Park R (2000) Analytical modelling of infilled frame structures—a general review. Bull N Z Soc Earthq Eng 33(1):30–47
Decreto Ministeriale (2017) Linee Guida per la Classificazione del Rischio Sismico delle Costruzioni—58/2017, Il ministero delle infrastrutture e dei trasporti. Rome
Del Gaudio C, De Martino G, Di Ludovico M, Manfredi G, Prota A, Ricci P, Verderame GM (2017) Empirical fragility curves from damage data on RC buildings after the 2009 L'Aquila earthquake. Bull Earthq Eng 15(4):1425–1450. https://doi.org/10.1007/s10518-016-0026-1
Dipartimento della Protezione Civile (2013) Scheda di 1° livello di rilevamento danno, pronto intervento e agibilità per edific ordinari nll'emergenza post-sismica. http://www.protezionecivile.gov.it/resources/cms/documents/scheda_AeDES_07_2013_corretta_.pdf
Dolce M, Manfredi G (2015) Libro bianco sulla ricostruzione privata fuori dai centri storici nei comuni colpiti dal sisma dell'Abruzzo del 6 aprile 2009. Doppiavoce, Napoli
EERI (2009) The Mw = 6.3 Abruzzo, Italy, Earthquake of 6 April 2009
Elnashai AS, Pinho R (1998) Repair and retrofitting of RC walls using selective techniques. J Earthq Eng 2(4):525–568. https://doi.org/10.1080/13632469809350334
Elwood KJ, Marquis F, Kim JH (2015) Post-earthquake assessment and repairability of RC buildings: lessons from Canterbury and emerging challenges. In: Proceedings of the tenth pacific conference on earthquake engineering, Sydney, Australia
EN 1998–1:2004 (2004) Eurocode 8: design of structures for earthquake resistance—part 1: general rules, seismic actions and rules for buildings. EN 1998-1:2004, Brussels
Fajfar P (2000) A nonlinear analysis method for performance-based seismic design. Earthq Spectra 16(3):573–592. https://doi.org/10.1193/1.1586128
Fardis MN (2017) Impact of experimental research on the Eurocode 8 provisions for RC structures. In: 7th international conference on advances in experimental structural engineering, Pavia, Italy
FEMA P58-1 (2012) Seismic performance assessment of buildings: volume 1—methodology (P-58-1). FEMA P58-1, Washington, DC

FEMA P58-3 (2012) Seismic performance assessment of buildings volume 3—performance assessment calculation tool (PACT) version 2.9.65 (FEMA P-58-3.1). FEMA P58-3, Washington, DC
FEMA P695 (2009) Quantification of building seismic performance factors. FEMA P695, Washington, DC
Filiatrault A, Sullivan T (2014) Performance-based seismic design of nonstructural building components: the next frontier of earthquake engineering. Earthq Eng Eng Vib 13(1):17–46. https://doi.org/10.1007/s11803-014-0238-9
Galli M (2006) Evaluation of the seismic response of existing RC frame buildings with masonry infills. M.Sc. thesis, IUSS Pavia, Italy
Gokkaya BU, Baker JW, Deierlein GG (2016) Quantifying the impacts of modeling uncertainties on the seismic drift demands and collapse risk of buildings with implications on seismic design checks. Earthq Eng Struct Dyn 45(10):1661–1683. https://doi.org/10.1002/eqe.2740
Hak S, Morandi P, Magenes G, Sullivan TJ (2012) Damage control for clay masonry infills in the design of RC frame structures. J Earthq Eng 16(sup1):1–35. https://doi.org/10.1080/13632469.2012.670575
Haselton CB, Liel AB, Taylor Lange S, Deierlein GG (2008) Beam-column element model calibrated for predicting flexural response leading to global collapse of RC frame buildings. PEER Report 2007/03, Berkeley, California
Ibarra LF, Medina RA, Krawinkler H (2005) Hysteretic models that incorporate strength and stiffness deterioration. Earthq Eng Struct Dyn 34(12):1489–1511. https://doi.org/10.1002/eqe.495
ISTAT (2011) Censimento della popolazione e delle abitazioni 2011. Censimento Popolazione Abitazioni. http://dati-censimentopopolazione.istat.it/Index.aspx# (25 Oct 2016)
Kazantzi AK, Vamvatsikos D (2015) Intensity measure selection for vulnerability studies of building classes. Earthq Eng Struct Dyn 44(15):2677–2694. https://doi.org/10.1002/eqe.2603
Kohrangi M, Vamvatsikos D, Bazzurro P (2016) Implications of intensity measure selection for seismic loss assessment of 3-D buildings. Earthq Spectra 32(4):2167–2189. https://doi.org/10.1193/112215eqs177m
Kohrangi M, Bazzurro P, Vamvatsikos D, Spillatura A (2017) Conditional spectrum-based ground motion record selection using average spectral acceleration. Earthq Eng Struct Dyn. https://doi.org/10.1002/eqe.2876
Krawinkler H (2005) Van nuys hotel building testbed report: exercising seismic performance assessment. PEER Report 2005/11, Berkeley, California
McKenna F, Fenves G, Filippou FC, Mazzoni S (2000) Open system for earthquake engineering simulation (OpenSees). http://opensees.berkeley.edu/wiki/index.php/Main_Page
Melo J, Varum H, Rossetto T (2015) Experimental cyclic behaviour of RC columns with plain bars and proposal for Eurocode 8 formula improvement. Eng Struct 88:22–36. https://doi.org/10.1016/j.engstruct.2015.01.033
Montaldo V, Meletti C (2007) Valutazione del valore della ordinata spettrale a 1sec e ad altri periodi di interesse ingegneristico. Progetto DPC-INGV S1, Deliverable D3. http://esse1.mi.ingv.it/d3.html
Morales E, Filiatrault A, Aref A (2017) Sustainable and low cost room seismic isolation for essential care units in developing countries. In: 16th world conference on earthquake engineering, Santiago, Chile
NTC (2008) Norme Tecniche Per Le Costruzioni. NTC, Rome
O'Connor JS, Morales E (2016) Reconnaissance of damaged structures after the 2016 Muisne–Ecuador earthquake (presentation). State University of New York at Buffalo, Buffalo, NY. http://gsa.buffalo.edu/eeri/wp-content/uploads/sites/41/2016/08/Enrique_OConnor_Seminar_Presentation.pdf
O'Reilly GJ (2016) Performance-based seismic assessment and retrofit of existing RC frame buildings in Italy. Ph.D. thesis, IUSS Pavia, Italy
O'Reilly GJ, Sullivan TJ (2015) Influence of modelling parameters on the fragility assessment of PRE-1970 Italian RC structures. In: COMPDYN 2015—5th ECCOMAS thematic conference on computational methods in structural dynamics and earthquake engineering
O'Reilly GJ, Sullivan TJ (2017a) Quantification of modelling uncertainty in existing Italian RC frames. Earthq Eng Struct Dyn (**in press**)
O'Reilly GJ, Sullivan TJ (2017b) Modelling uncertainty in existing Italian RC frames. In: COMPDYN 2017—6th international conference on computational methods in structural dynamics and earthquake engineering, Rhodes Island, Greece
O'Reilly GJ, Sullivan TJ (2017c) Modelling techniques for the seismic assessment of existing Italian RC frame structures. J Earthq Eng. https://doi.org/10.1080/13632469.2017.1360224
O'Reilly GJ, Perrone D, Fox MJ, Lanese I, Monteiro R, Filiatrault A, Pavese A (2017a) System identification and seismic assessment modelling implications for Italian school buildings. Earthq Eng Struct Dyn (**accepted**)
O'Reilly GJ, Perrone D, Fox MJ, Monteiro R, Filiatrault A (2017b) Seismic vulnerability of existing school buildings in Italy. Eng Struct (**accepted**)

O'Reilly G, Monteiro R, Perrone D, Lanese I, Fox M, Pavese A, Filiatrault A (2017c) System identification and structural modelling of Italian school buildings. In: Caicedo J, Pakzad S (eds) Conference proceedings of the society for experimental mechanics series on dynamics of civil structures, vol 2. Springer International Publishing, pp 301–303

Pampanin S, Calvi GM, Moratti M (2002) Seismic behaviour of RC beam-column joints designed for gravity loads. In: 12th European conference on earthquake engineering, London, UK

Porter KA, Beck JL, Shaikhutdinov RV (2004) Simplified estimation of economic seismic risk for buildings. Earthq Spectra 20(4):1239–1263. https://doi.org/10.1193/1.1809129

Priestley MJN, Calvi GM, Kowalsky MJ (2007) Displacement based seismic design of structures. IUSS Press, Pavia

Ramirez CM, Miranda E (2009) Building specific loss estimation methods and tools for simplified performance based earthquake engineering. Blume report no. 171, Stanford, CA

Regio Decreto (1939) Norme per l'esecuzione delle opere conglomerato cementizio semplice od armato—2229/39. Rome

Rossetto T, Elnashai A (2003) Derivation of vulnerability functions for European-type RC structures based on observational data. Eng Struct 25(10):1241–1263. https://doi.org/10.1016/s0141-0296(03)00060-9

Sassun K (2014) A parametric investigation into the seismic behaviour of window glazing systems. M.Sc. thesis, IUSS Pavia, Italy

Sassun K, Sullivan TJ, Morandi P, Cardone D (2015) Characterising the in-plane seismic performance of infill masonry. Bull N Z Soc Earthq Eng 49(1):100

SEAOC (1995) Vision 2000: performance-based seismic engineering of buildings. SEAOC, Sacramento

Taghavi S, Miranda E (2003) Response assessment of nonstructural building elements. PEER Report 2003/05, Berkeley, California

Vamvatsikos D, Cornell CA (2002) Incremental dynamic analysis. Earthq Eng Struct Dyn 31(3):491–514. https://doi.org/10.1002/eqe.141

Vamvatsikos D, Cornell CA (2005) Direct estimation of seismic demand and capacity of multidegree-of-freedom systems through incremental dynamic analysis of single degree of freedom approximation. J Struct Eng 131(4):589–599. https://doi.org/10.1061/(asce)0733-9445(2005)131:4(589)

Vona M, Masi A (2004) Resistenza sismica di telai in c.a. progettati con il R.D. 2229/39. XI Congresso Nazionale "L'Ingegneria Sismica in Italia", Genova, Italia

Welch DP, Sullivan TJ, Calvi GM (2014) Developing direct displacement-based procedures for simplified loss assessment in performance-based earthquake engineering. J Earthq Eng 18(2):290–322. https://doi.org/10.1080/13632469.2013.851046